ANALYSIS OF CONTINUOUS FOLDED PLATE SURFACE

by

Frederick William Beaufait, B.S., M.S.C.E.

Thesis submitted to the Graduate Faculty of the

Virginia Polytechnic Institute

in candidacy for the degree of

DOCTOR OF PHILOSOPHY

in

Civil Engineering

June 4, 1965

Blacksburg, Virginia

TABLE OF CONTENTS

LIST OF FIGURES

LIST OF FIGURES - CONTINUED

LIST OF TABLES

ANALYSIS OF CONTINUOUS FOLDED PLATE SURFACE

I INTRODUCTION

The folded plate surface is a shell developed by a series of flat plates, monolithic in the longitudinal direction and supported by transverse diaphragms or bents (Figure 1). Because the folded plate surface offers numerous architectural, structural and economical solutions to the problem of large, clear spans, interest in this structural system has increased within the past ten years. Although this type of structure has been used primarily in the construction of long-span roofing and flooring systems, the folded plate surface has many other possible applications.

Design techniques have been developed but only for the single-span folded plate surface. This dissertation presents an extension of the folded plate theory for the analysis of the continuous folded plate surface. In addition, a computer program written for the solution of selected folded plate surfaces is described and experimental verification of the folded plate theory for single and continuous span surfaces is established.

A. HISTORICAL BACKGROUND

In 1930, one of the first papers to present a method of

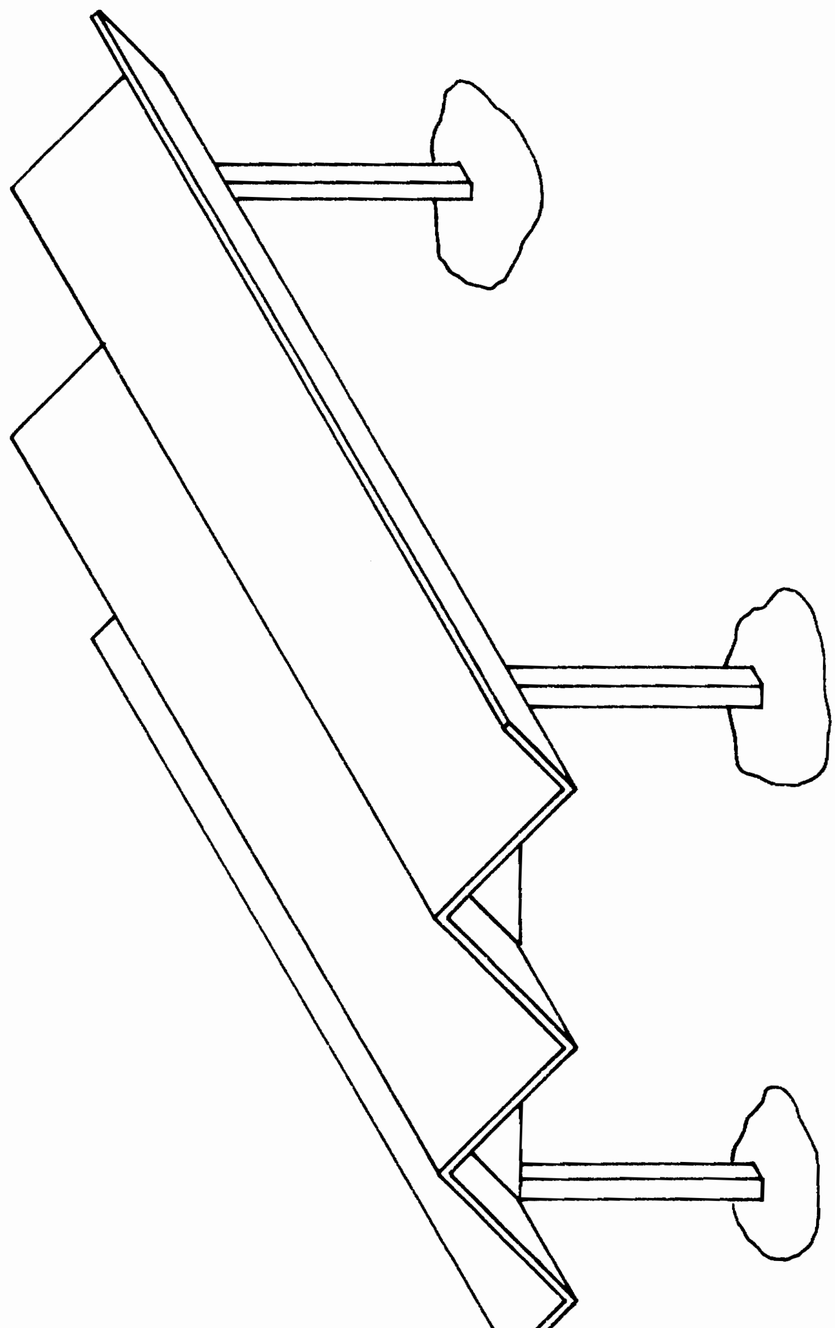

FIGURE I. FOLDED PLATE SURFACE

analysis for the folded plate surface was written in Germany by G. Ehlers[1]. The folded plate theory which was presented in this paper neglected the relative displacements of the fold lines and assumed also that the plates were hinged along the fold lines. The folded plate theory was further developed by H. Craemer[2] to account for the transverse moments which arise at the fold lines due to the continuity which is established by construction.

In 1932, the folded plate theory was expanded to include the effects of the relative displacement of the fold lines with the publication of papers in the German literature by E. Gruber[3] and G. Gruening[4]. Since the proposed method of analysis involved the solution of simultaneous, fourth order differential equations for the determination of the displacements of the fold lines, it proved to be a rather cumbersome technique. However, in 1936 the technique was simplified by W. Z. Vlassow[5] by applying linear, algebraic equations to determine the longitudinal stresses and ridge movements.

In 1947, the folded plate theory was first published in American literature in a paper by G. Winter and M. Pei[6]. Although this paper dealt with the theory that neglected the relative movement of the fold lines, it did introduce a technique of relaxation similar to the moment distribution procedure for determining the longitudinal stresses.

In 1954, I. Gaafar[7] presented a paper in which an iteration procedure was developed to account for the relative movement of the fold lines. In this paper, Gaafar pointed out the danger of neglecting the effects of the relative movements of the fold lines on stresses, forces and moments which are developed in the folded plate surface. In considering the relative movements of the fold lines, the technique which was presented in this paper had one disadvantage in that the iteration procedure would diverge rather than converge toward a final solution if the deflection angles between adjacent plates were not of sufficient magnitude.

In 1958, H. Simpson[8] further simplified the folded plate theory that accounted for relative movement of fold lines by introducing a technique similar to the moment distribution procedure for the analysis of multi-degree of freedom systems. Employing the familiar methods of structural analysis, the technique involved the solution of $n - 2$ simultaneous equations (where n is the number of plates of the folded plate surface). Thus by eliminating the need to solve a large number of simultaneous, differential or algebraic equations and using procedures familiar to the engineer, this technique has become the basis for present methods of analysis of the folded plate surface.

Within recent years there have been several significant techniques presented for the analysis of the folded plate surface. Many of the techniques, such as those by Portland Cement Association[9], Meek[10], Barker[11] and Scordelis[12,13], have been presented in a form that could be programmed effectively for the electronic digital computer.

With few exceptions, the various techniques for the solution of the folded plate surface have been limited to the simply supported, single-span surface. However, Yitzhaki[14], in his book concerning shell roofs, has considered the problem of the continuous folded plate surface. Using the method of "particular loading" which he has developed[14,15], each span of the continuous surface is considered individually, assuming idealized end conditions of being fixed, free or simply supported. Because the continuous structure is not treated as a unit and the continuity of the surface over the supports is unduly restrained by fixity, the method of analysis offers only an approximate solution of the behavior of the folded plate. Sharma and Goyal[16] have also considered the analysis of the continuous folded plate surface employing the same technique of studying each span individually with idealized end conditions.

In the numerous techniques for analyzing the folded plate surface, the compatibility in the behavior of the surface in both the transverse and longitudinal direction at the fold lines has been provided for at one section in the span and is assumed to be satisfied at all other sections. In order to satisfy the compatibility at all sections, the deflected shape of the surface and the distribution of the forces and moments are expressed in terms of an idealized curve, usually as a Fourier series. Although this idealization yields acceptable results for the simple span folded plate surface, it does not define the exact distribution of stresses and does not lend itself easily to the analysis of the continuous folded plate surface as a single unit. In analyzing the continuous folded plate, the exact distribution of stresses, forces and moments, as well as plate deflections, must be calculated at all sections in the spans to provide overall compatibility.

B. PURPOSE

The purpose of this dissertation is (1) to present a general method of analysis of simple-span and continuous-span folded plate surfaces that will insure compatibility at all points and continuity over the transverse supports, (2) to describe a computer program employing this technique for the solution of simple-span and continuous-span folded plate surfaces, with or without overhangs at the ends, for three load conditions, and (3) to present the results of an experimental study of four aluminum models of a folded plate surface.

Techniques for the analysis of single-span folded plate surfaces have been fairly well established. With these as a basis, a general method of analysis is developed here for continuous-span folded plate surfaces which provides for complete continuity over the transverse supports. Prior to the development of the electronic digital computer, such a general solution would have been somewhat impractical because of the tremendous number of computations involved. With this thought in mind, representative structures have been considered and a computer program has been developed to obtain their solution.

Although there have been numerous papers on the analysis of the simply supported folded plate surface, there is very little information available on the experimental verification of the folded plate theory. In 1954, I. Gaafar[7] conducted some experimental work on an aluminum hipped plate structure which yielded fair correlation with the folded plate theory he introduced; and Scordelis[13] has presented the results which were obtained in 1961 from a study of a simple-span, aluminum, folded plate model consisting of three north-light shells. In order to obtain additional experimental verification of the analysis of the simply supported folded plate surface and to establish verification of the general method of analysis of continuous folded plate surfaces, an experimental investigation of four aluminum models was made. The results of this investigation offers excellent verification of the proposed general method of analysis.

II ASSUMPTIONS

The analysis of the behavior of the folded plate surface is based upon the following assumptions:

1. The material is homogeneous, uncracked and not strained beyond its elastic limit; strain is proportional to stress (Hooke's Law); and strain varies linearly across the width of each plate.

2. The longitudinal joints at the fold lines are monolithic and unseparated throughout their entire lengths. The plates are continuous without holes.

3. The supporting diaphragms or bents are infinitely rigid in their plane and perfectly flexible normal to their plane.

4. The change in the geometry of the loaded surface resulting from the actual deflection is small relative to the overall configuration of the surface. Thus, the equations of equilibrium are based on the geometry of the undeflected surface.

5. Each plate is relatively long compared to its width (length to width ratio equal to, say, three or more). Thus, in bending normal to its plane, the plate is assumed to behave as a one-way slab; the stresses induced by longitudinal slab action and by twisting of the plates is neglected.

6. Longitudinal stresses in each plate vary linearly across the width.

7. Deformations resulting from shearing stresses and normal, transverse stresses in each plate have a negligible effect on the deformation on the surface.

These are the assumptions customarily made in analyzing the folded plate surface[17]. However, there are some limitations which result from these basic assumptions.

Where the deflection angle between adjacent plates is small, it is necessary to check the position of the deflected surface relative to the no-load position of the surface to assure validity of the equations of equilibrium (Assumption 4, above). (The deflection angle between adjacent plates should not be less than 15°).

Linearity of longitudinal stresses (Assumption 6, above) and negligible shear deformations (Assumption 7, above) are not valid assumptions when the span to width ratios are small (smaller than three for longitudinal stresses and five for shear deformations for simply supported surfaces). Deformations resulting from the transverse, normal stresses caused by walls or other external restraints should be investigated where the plate is not permitted to translate freely in its plane. The effects of two-way slab action should not be overlooked in the vicinity of the supporting diaphragms or bents (Assumption 5, above).

III SIGN CONVENTION

A set of rectangular coordinate axes with the origin at the left edge of the extreme left plate is established for the transverse section of the folded plate surface (Figure 2a). The individual plates of the surface are identified by numbers (1,2,3,.....) beginning with the cantilever edge plate on the left of the transverse section and the fold lines (plate edges) are identified by letters (A,B,C,.....) beginning at the origin (Figure 2a).

The basic sign convention established for the general analysis of the folded plate surface and employed in the formulation of the computer program for the analysis is as follows:

1. The assumed positive direction for the surface loads (P_i^N , P_i^T) and angles between adjacent plates (a_i) and the rectangular coordinate system for a transverse section is shown in Figure 2a.
2. The transverse moments (TM_j) are assumed positive when causing tension stresses in the bottom fiber of the surface (Figure 2b).
3. The in-plane plate loads (F_{ji}) are assumed positive when acting in a direction toward the prior alphabetical edge (Figure 4b).
4. The longitudinal, in-plane bending moments (M_{im}) are assumed positive when causing the prior alphabetical edge to be in tension and the latter alphabetical edge

to be in compression (Figure 6).

5. The edge shear forces (N_{jm}) are assumed positive when causing stresses of the same sign as those caused by the positive longitudinal, in-plane bending moments (Figure 6a).

6. The axial plate forces (P_{im}) are assumed positive when causing tensile longitudinal fiber stresses and negative when causing compressive longitudinal fiber stresses.

7. The tensile longitudinal fiber stresses (f_{jm}) are assumed to be positive and compressive longitudinal fiber stresses are assumed to be negative (Figure 6b).

8. The in-plane plate deflections (d_{im}) are assumed positive when movement is in a direction of the prior alphabetical edge (Figure 7).

9. The plate rotation (r_i) is assumed positive when in a counter-clockwise direction as shown in Figure 8.

IV GENERAL METHOD OF ANALYSIS

The general method of analysis as presented here is developed for the solution of single or continuous span folded plate surfaces, with general end conditions, for any loading. By considering the folded plate surface as a single, longitudinal unit throughout the analysis, the continuity of the surface is maintained over the transverse supports. Within the limitations of the assumptions, this method yields an "exact" solution of the structural action of the folded plate surface based upon a difference technique in which the surface is divided into segments: compatibility of the surface is insured at the center of each finite segment along the span and over the supports. This method of analysis is basically similar to methods presented by H. Gesund[18] and H. Simpson[8] for the analysis of the single-span, simply supported folded plate surface except that the true deflected shape is used rather than an assumed sinusoidal deflected shape.

The basic structural action of the folded plate surface is assumed to consist of two parts. The first is a one-way slab action in the transverse direction in which the support of all normal surface loads is transferred to the longitudinal fold lines (Figure 3 and 4). The second is the longitudinal, in-plane bending (beam action) of the plates in which the edge loads, acting along the fold lines, and in-plane surface loads are transferred through the plates to the supports (Figure 5).

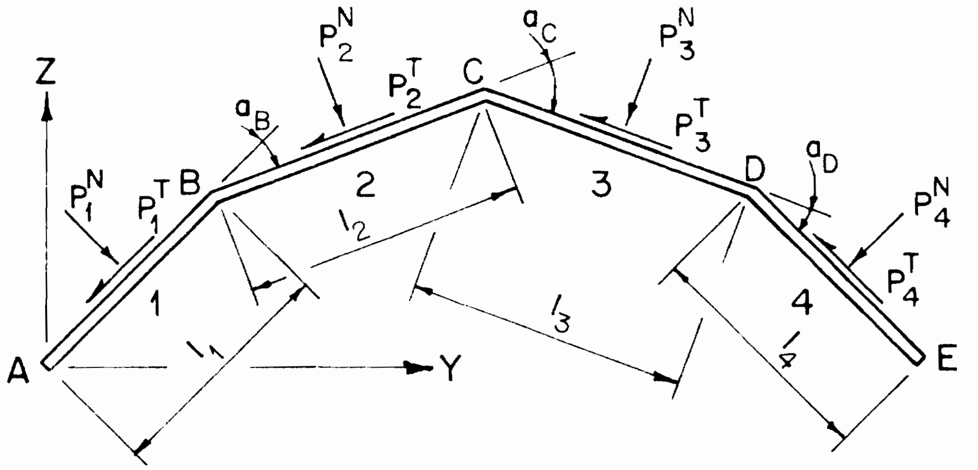

a) TRANSVERSE SECTION

All forces, moments, reactions, loads and angles are assumed positive as shown.

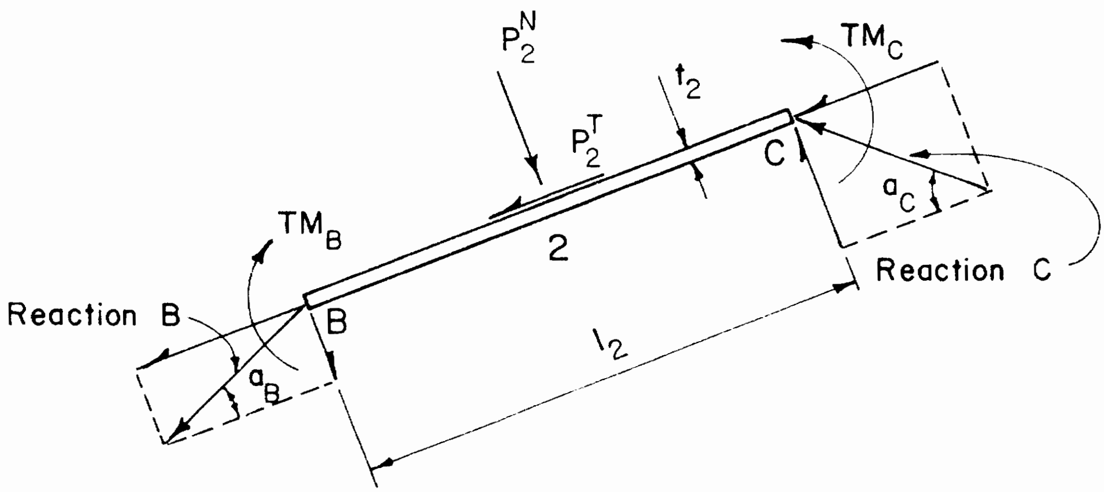

b) FORCES ON PLATE 2

FIGURE 2. SIGN CONVENTION (TRANSVERSE)

The general method of analysis consists of three phases; (1) a membrane analysis of individual plates separated at the fold lines, (2) the analysis of arbitrary plate rotations, and (3) the development of the final solution combining (1) and (2) to restore continuity at the fold lines. The steps to be carried out in this analysis of the folded plate surface are as follows:

(One-way Slab Action)

1. Establish the normal and tangential components of the applied surface load (P_i^N , P_i^T) for each plate (Figure 2). The applied surface load is assumed to be uniformly distributed in the longitudinal direction. For other distributions of load, the procedure can be modified as necessary. If the surface load is applied along the fold lines, the analysis begins with Step 4, below.

2. Consider a transverse strip of unit width and for that strip assume that the interior fold lines are restrained against translation by imaginary supports (Figure 3), calculate the transverse moments (TM_j) at the interior fold lines produced by the normal components of the plate loads (Figure 2), and determine the restraining forces (R_j) produced by the imaginary supports (Figure 3). These transverse moments (TM_j) and restraining forces (R_j) are applied longitudinally along the fold lines in proportion to the longitudinal distribution of the applied surface load.

(Beam Action)

3. Remove the imaginary supports and apply loads (R_j') which are

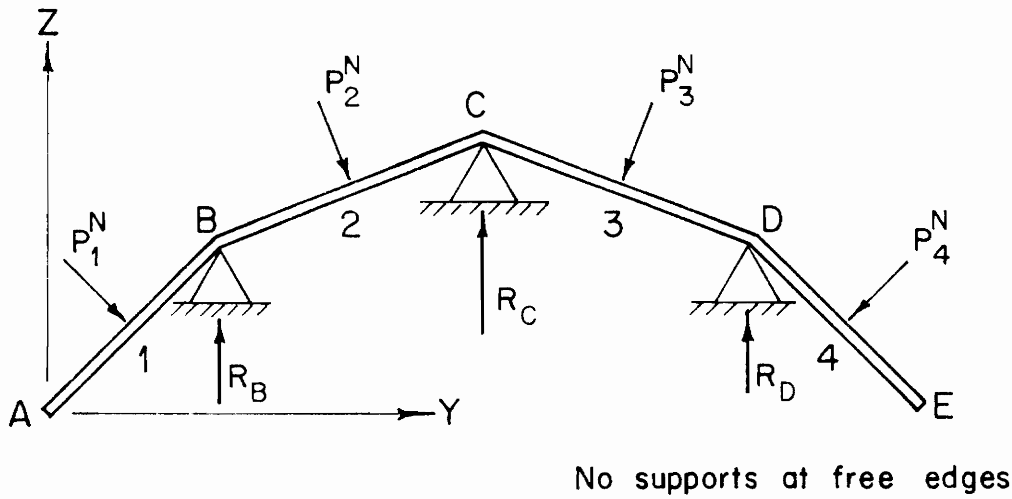

FIGURE 3. REACTIONS OF IMAGINARY SUPPORTS

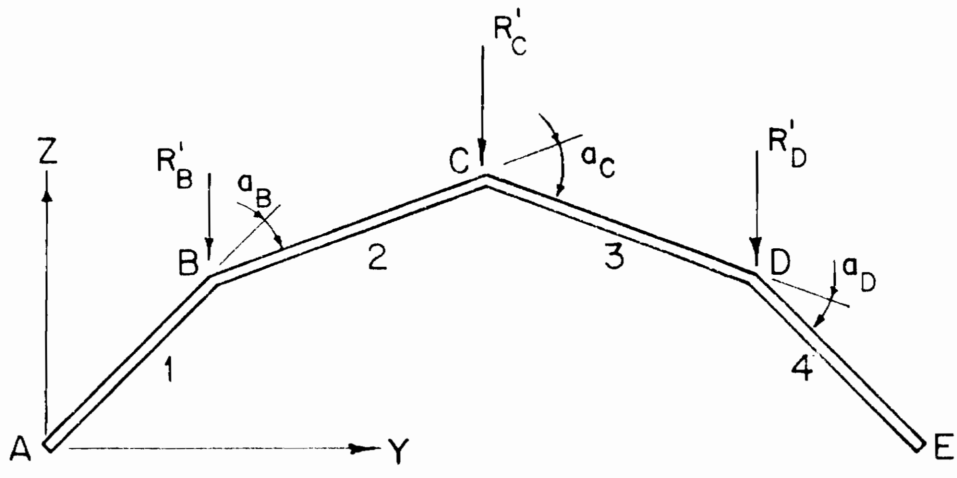

a) EDGE LINE LOADS

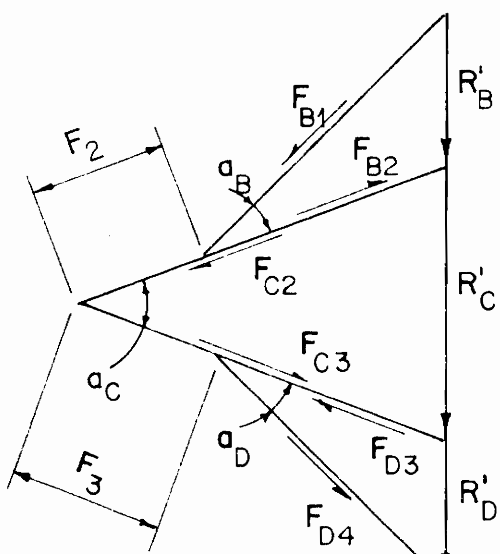

b) COMPONENTS OF EDGE LINE LOADS IN PLANE OF PLATES

FIGURE 4. PLATE LOADING

equal and opposite to the computed restraining forces (R_j), at the corresponding interior fold lines (Figure 4a).

4. Assume now that the plates in place are temporarily separated along their fold lines, resolve the loads (R'_j) into their respective component forces (F_{ji}) in the planes of the adjacent plates (Figure 4b), and calculate the total, in-plane plate loads (PL_i) for each plate by summing these forces (F_{ji}) and the tangential components of the applied surface loads (P_i^T) in the plane of the plates. These loads are then applied longitudinally along each plate producing beam action (Figure 5).

Divide each span of the folded plate surface into transverse segments of equal length (Figure 5). The length of segments within the different spans does not have to be the same. It should be noted that the accuracy of the analysis is dependent upon the size of segments chosen. Smaller segments produce greater accuracy.

5. Assume that each plate acts independently, calculate the longitudinal bending moments in the plates at the supports (SM_{ik}) due to the in-plane bending (beam action) of the plates and determine the corresponding longitudinal, in-plane bending moments (M_{im}) that occur at the center of each segment established above.

6. In order to maintain continuity at the fold lines, the longitudinal stresses (f_{jm}) at the common edges of adjacent plates must be equal. Where the solution of Step 5, above, results in unequal

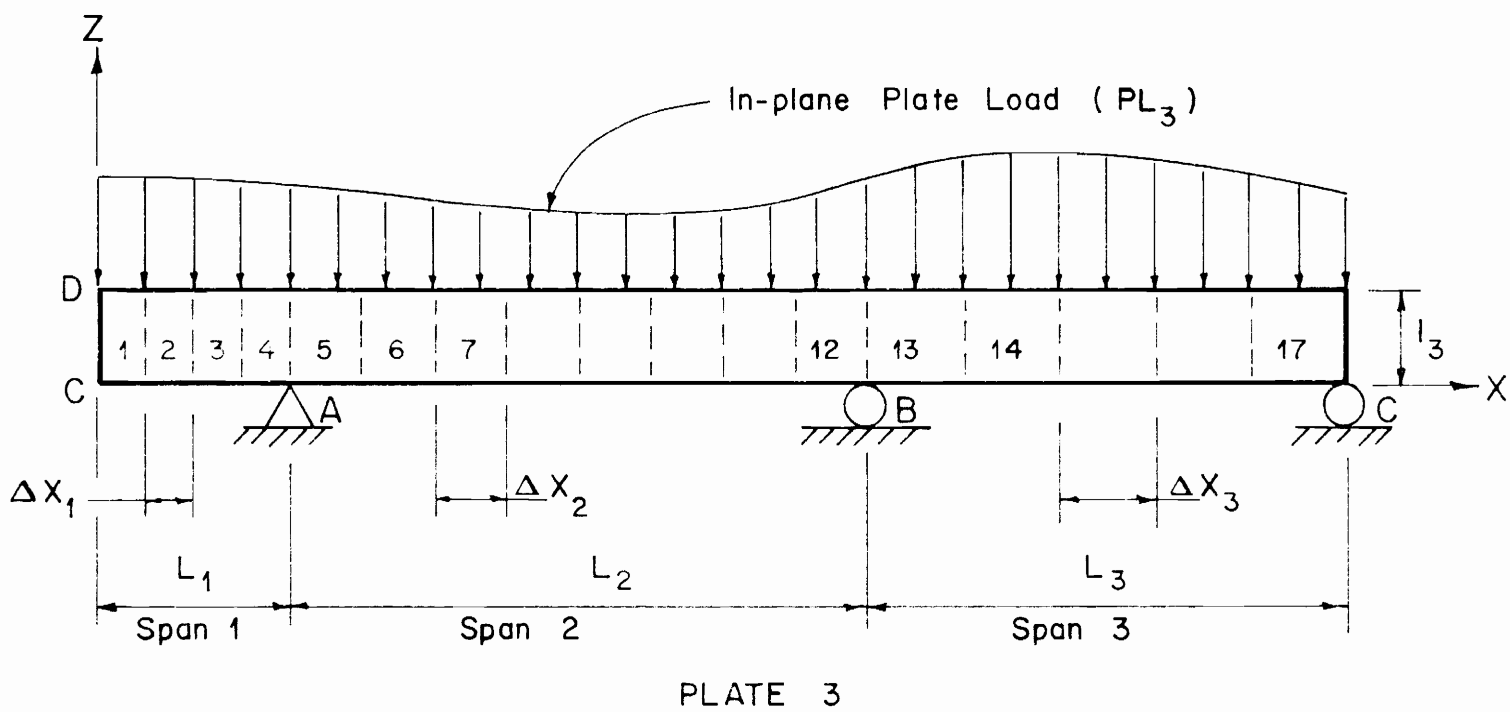

FIGURE 5. TYPICAL PLATE - LONGITUDINAL SPAN

longitudinal stresses, they can be made equal by applying corrective shearing stresses (s_j) to both plates along their common edges (Figure 6). These shearing stresses must be equal and opposite at the common fold lines. Then for any transverse section, the equilibrium force (N_{jm}) caused by the shear stress (s_j) along the fold line is calculated as

$$N_{jm} = \int_0^x s_j \, t_j \, dx_m \ ,$$

where t_j is the thickness of the plates at the fold lines.

The longitudinal stresses at the edges of each plate for any transverse section at the center of any given segment can be expressed in terms of the edge shear forces (N_{jm}), defined above, and the longitudinal, in-plane bending moments (M_{im}), established in Step 5. Considering plate 3 (Figure 2a), the equation for the longitudinal stress at edge D, segment 6, would appear as

$$f_{D,6} = (N_{D,6} - N_{C,6}) \frac{1}{l_3 \, t_3} + (M_{3,6} + (N_{D,6} + N_{C,6})) \frac{l_3}{2 \, I_3} \ ,$$

where l_3 is the plate length, t_3 is the thickness and I_3 is the moment of inertia (Figure 6). By equating the longitudinal stresses (f_{jm}) at common fold lines, the longitudinal stresses (f_{jm}) can be eliminated and a set of equations in terms of N_{jm} and M_{im} can be solved simultaneously for the edge shear forces (N_{jm}).

These edge shear forces (N_{jm}) produce additional in-plane bending moments in each plate which for plate 3, segment 6, would

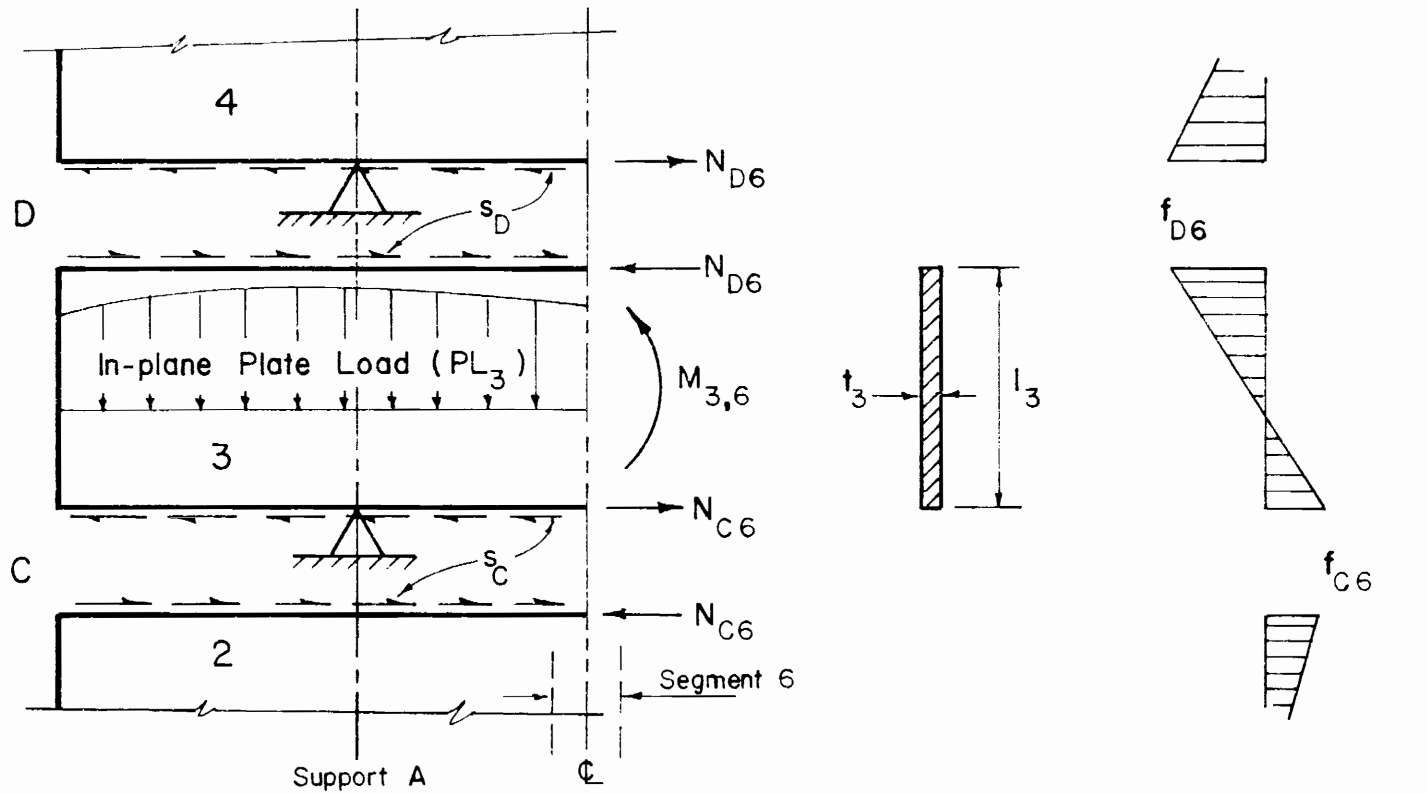

a) LONGITUDINAL IN-PLANE FORCES, MOMENTS AND LOADS

b) LONGITUDINAL IN-PLANE STRESSES

All forces, moments and loads are assumed positive as shown. Tension stresses are assumed positive.

FIGURE 6. SIGN CONVENTION (LONGITUDINAL)

equal

$$(N_{D,6} + N_{C,6}) \frac{l_3}{2} \quad .$$

Thus, the total in-plane, longitudinal bending moment (LM_{im}) for plate 3, segment 6, becomes

$$LM_{3,6} = M_{3,6} + (N_{D,6} + N_{C,6}) \frac{l_3}{2} \quad ,$$

where $M_{3,6}$ is defined in Step 5, above.

7. Define the "conjugate beam" for each plate independently, apply the appropriate elastic loads ($\frac{LM_{im}}{E\ I_i}$) and calculate the deflections (d_{im}) along each plate at the center of each segment.

8. For convenience of computation, nondimensionalize the deflections (d_{im}) calculated for each plate by dividing by the value of deflection at a selected transverse segment (reference segment). The same segment must be used as the reference segment for all plates.

Steps 1 to 8 constitute the "membrane" (determinate) analysis of the folded plate surface. In order to obtain the complete solution, it is necessary to correct for the relative separations of the fold lines resulting from the membrane analysis. This correction is made by translation and rotation of the plates which, in turn, introduce additional transverse moments, longitudinal, in-plane moments and edge shear forces. The technique used to make this correction is similar to a sway correction in the solution of a multi-story building frame by the moment distribution method; the entire folded plate surface is analyzed for an arbitrary rotation (r_i') of each plate independently, as follows:

9. Consider a unit transverse strip as in Step 2, induce an arbitrary plate rotation (r_i') of one plate (Figure 8) and determine the resulting transverse moments and edge loads as in Step 2. Apply these moments and edge loads longitudinally along the fold lines in proportion to the nondimensionalized deflections (Step 9) of the plate rotated. Repeat the operation of Steps 3 through 7 to obtain the longitudinal forces, moments and deflections for the arbitrary rotation imposed.

This procedure is repeated for each plate across the transverse section (except cantilever edge plates).

10. At any given transverse section taken at the center of a segment, the final in-plane deflection (d''_{im}) of each plate is now expressed in terms of the in-plane deflections (d_{im}) of the membrane analysis and the sum of k_n times the in-plane deflections (d^n_{im}) established for each independent plate rotation (r_i'), where k_n are constant coefficients dependent upon the arbitrary rotations (r_i') and n denotes the particular independent plate rotation being considered. For plate 3, segment 6, this equation would be written as

$$d''_{3,6} = d_{3,6} + k_2 d^2_{3,6} + k_3 d^3_{3,6} + \cdots\cdots\cdots\cdots + k_n d^n_{3,6} \quad .$$

11. Considering the geometry of the folded plate surface, the actual rotation (r_i) of each plate can be expressed in terms of the final in-plane deflections (d''_{im}) of the plates. For plate 3, segment 6, the actual rotation would be expressed as

$$r_3 = \frac{1}{l_3} \left(d''_{2,6}\csc(a_C) - d''_{3,6}\left(\cot(a_C) + \cot(a_D) \right) + d''_{4,6}\csc(a_D) \right)$$

where a_C and a_D (a_j) are the deflection angles between adjacent plates (Figure 7). Also, the actual rotation (r_i) of each plate can be expressed as a function of the arbitrary rotation imposed on that plate in Step 9. For plate 3, segment 6, the expression would be written as

$$r_3 = k_3 r'_3$$

where k_3 is the constant coefficient k_n introduced in Step 10. Combining these two expressions for each plate and substituting for the values of final in-plane deflections (d''_{im}) established in Step 10, the resulting set of simultaneous equations is solved for the unknown coefficients k_n.

Steps 10 and 11 need only be carried out at one transverse section of the surface, preferably at the reference segment defined in Step 8. The resulting values of k_n can be applied at all transverse sections.

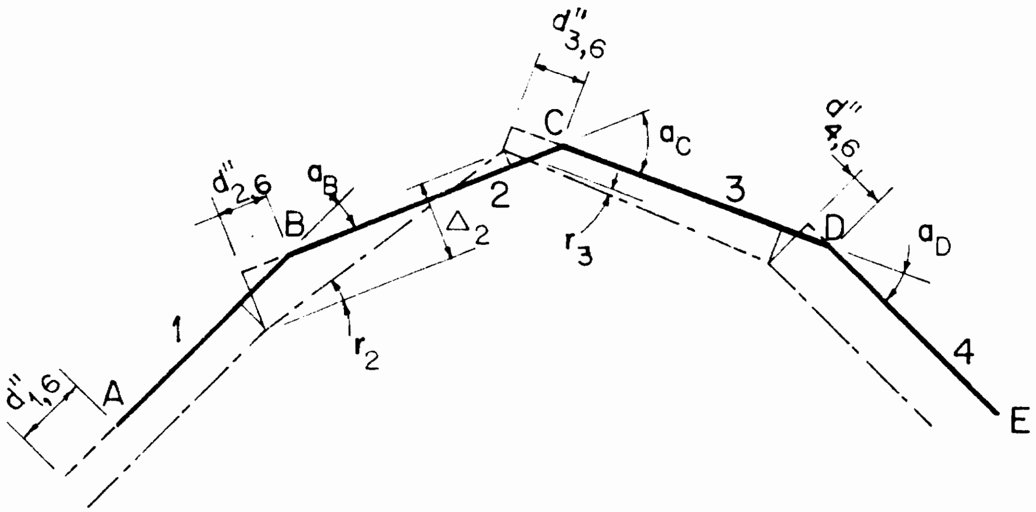

FIGURE 7. PLATE DEFLECTIONS AND ROTATIONS - SEGMENT 6

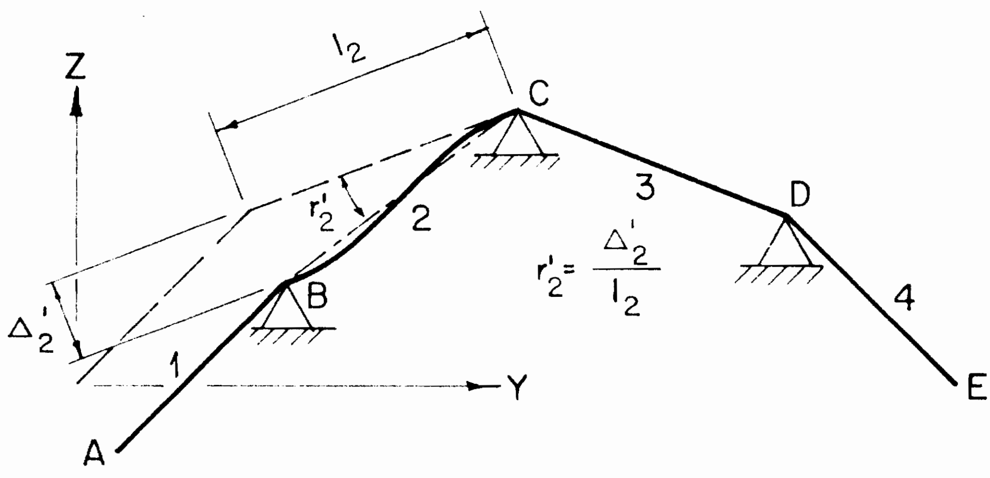

FIGURE 8. ARBITRARY PLATE ROTATION

12. The final solution of the folded plate surface, i.e., stresses (f''_{jm}), forces (N''_{jm}) and moments (TM''_{jm} , LM''_{im} , M''_{im} , SM''_{ik}), is the sum of the values from the membrane analysis plus the values from each rotational analysis times the appropriate constant coefficient:

$$f''_{jm} = f_{jm} + k_2 f^2_{jm} + k_3 f^3_{jm} + \cdots\cdots + k_n f^n_{jm} ,$$

$$N''_{jm} = N_{jm} + k_2 N^2_{jm} + k_3 N^3_{jm} + \cdots\cdots + k_n N^n_{jm} ,$$

$$TM''_{jm} = TM_{jm} + k_2 TM^2_{jm} + k_3 TM^3_{jm} + \cdots\cdots + k_n TM^n_{jm} ,$$

$$LM''_{im} = LM_{im} + k_2 LM^2_{im} + k_3 LM^3_{im} + \cdots\cdots + k_n LM^n_{im} ,$$

$$M''_{im} = M_{im} + k_2 M^2_{im} + k_3 M^3_{im} + \cdots\cdots + k_n M^n_{im} ,$$

$$SM''_{ik} = SM_{ik} + k_2 SM^2_{ik} + k_3 SM^3_{ik} + \cdots\cdots + k_n SM^n_{ik} .$$

V COMPUTER PROGRAM

It would be extremely time consuming to attempt the analysis of a continuous folded plate surface without the use of an electronic digital computer, not to mention the difficulty of avoiding computional errors. Once a satisfactory computer program has been developed, the computer reduces the work involved in the analysis to a matter of hours. The program described in this dissertation was written in Fortran language for the IBM 1620-60k computer. It is composed of three phases consistent with the general method of analysis as presented earlier: (1) membrane analysis, (2) analysis of arbitrary plate rotations and (3) final solution; and two subroutines: (1) matrix inversion and (2) matrix multiplication.

For the program, the necessary input data is as follows; (1) the number of longitudinal spans, (2) the number of plates, (3) a code indicating the type of load condition, (4) a code indicating the longitudinal support condition, (5) the coordinates of the fold lines (plate edges), (6) the longitudinal span lengths, (7) the number of transverse segments in each span, (8) the magnitude of loads, (9) the modulus of elasticity, and (10) the plate thicknesses.

The final output of the program consists of the following items: (1) the transverse moments (TM''_{jm}) at each fold line at the center of each segment, (2) the total in-plane plate loads (PL''_i) for each plate at the center of each segment, (3) the longitudinal moments (LM''_{im}) in each plate at the center of each segment and the longitudinal moments (SM''_{ik}) in each plate at the line of support, (4) the edge shear forces (N''_{jm}) at each fold line at the center of each segment and at the line of supports, (5) the total axial load (P''_{im}) in each plate at the center of each segment, (6) the longitudinal stresses (f''_{jm}) at each fold line at the center of each segment and at the line of supports, and (7) the in-plane plate deflections (d''_{im}) of the plates at the center of each segment.

The program is designed for the analysis of simply supported, single-span or continuous-span folded plate surfaces, with or without overhangs at the ends, under three load conditions: (1) uniformly distributed load over the entire horizontal projection of the surface, (2) uniformly distributed normal and/or tangential loads over each individual plate, and (3) uniform, vertical line loads applied along individual fold lines in each span. The program is limited to surfaces where no more than two plates meet at any fold line. Due to the limited capacity of the IBM 1620-60k computer, the size of the folded plate surface which can be studied is restricted to a maximum of twenty plates and four spans, including overhangs, with a maximum of twenty-eight segments.

Phase 1 of the program, the membrane analysis, is composed of five steps. Each of these steps represents a pass through the computer. The different steps, as well as the three phases, are connected by COMMON statements which establish the continuity of the program. In the first step the geometry of the folded plate surface is established and values are computed for normal and tangential components of a uniform load over the horizontal projection of the surface for each plate, load condition (1), above. The transverse slab moments and the in-plane plate loads are calculated in the second step and the longitudinal moments in each plate, resulting from the beam action of the individual plates, are computed in the third step. In the fourth step the compatibility of the longitudinal stresses at the fold lines is established, i.e., the magnitude of the edge shear forces is computed and the total longitudinal bending moments in each plate are determined. In the fifth and last step, the in-plane plate deflections of each plate are computed and the deflected shape of the surface is established.

Phase 2, the analysis of the folded plate surface for the arbitrary rotation of the individual plates, is composed of four steps which correspond to the second through fifth steps of Phase 1. The four steps of Phase 2 are repeated for the rotation of each plate across the transverse section (except cantilever edge plates).

Phase 3, which yields the final solution of the surface, is composed of three steps. In the first step the constant coefficients, k_n, which combine the arbitrary plate rotations and the membrane analysis are computed and in the second and third steps the final solution for the folded plate surface, i.e., stresses, forces, moments and deflections, is computed.

The organization of the computer program is given in the flow chart in Appendix B. This chart does not attempt to show the detailed operations of the program but rather the general procedure followed in the solution of a folded plate surface. One familiar with computer programming, structural analysis and elementary folded plate analysis will be able to produce a working program from the flow chart for the general solution of folded plates.

VI EXPERIMENTAL INVESTIGATION

Following the development of the general method of analysis of continuous folded plate surfaces, an experimental investigation was planned to provide the means for verification of the method. Two simply supported, single-span models were first tested to verify the testing techniques and measurements against accepted folded plate theory for the simple span, and then two models of continuous folded plate surfaces were tested to verify the stresses computed by the general method of analysis presented in Section IV. The models were analyzed theoretically as structures with their actual dimensions.

A. EXPERIMENTAL PROGRAM

The experimental program was organized to study the behavior of four individual folded plate structures and to collect experimental values of longitudinal and transverse stresses which could be compared with theoretical values.

The first model tested in this program (Model 1 - Figure 9) consisted of a three plate, simply supported, single-span surface, the simplest form of folded plate surface. Since this surface was statically determinate, i.e., there were no corrections for joint displacement required, the action of the structure was the same as that of a simple beam. This surface was selected because of its simplicity and reliability to act as predicted by known methods of analysis. The comparison of the theoretical and experimental

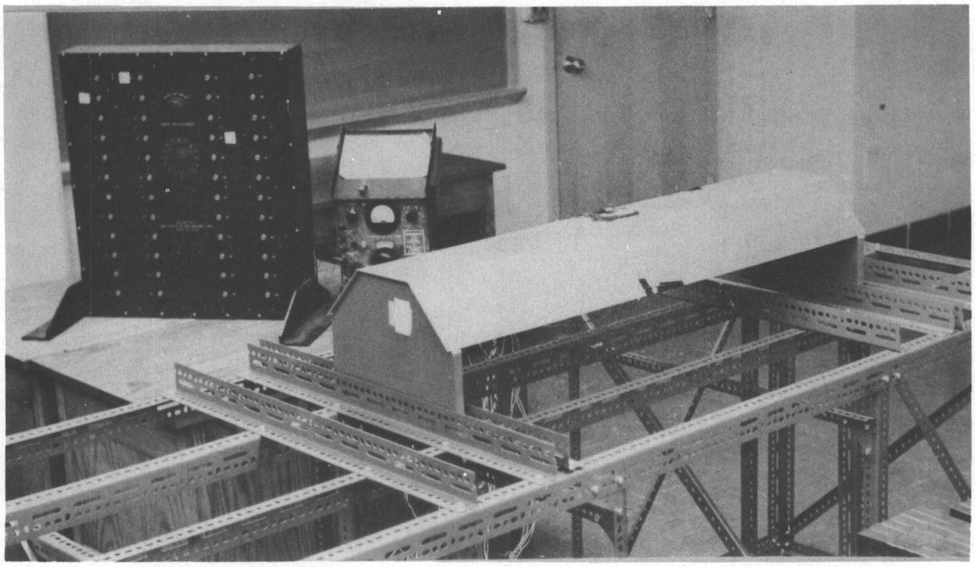

FIGURE 9. MODEL 1

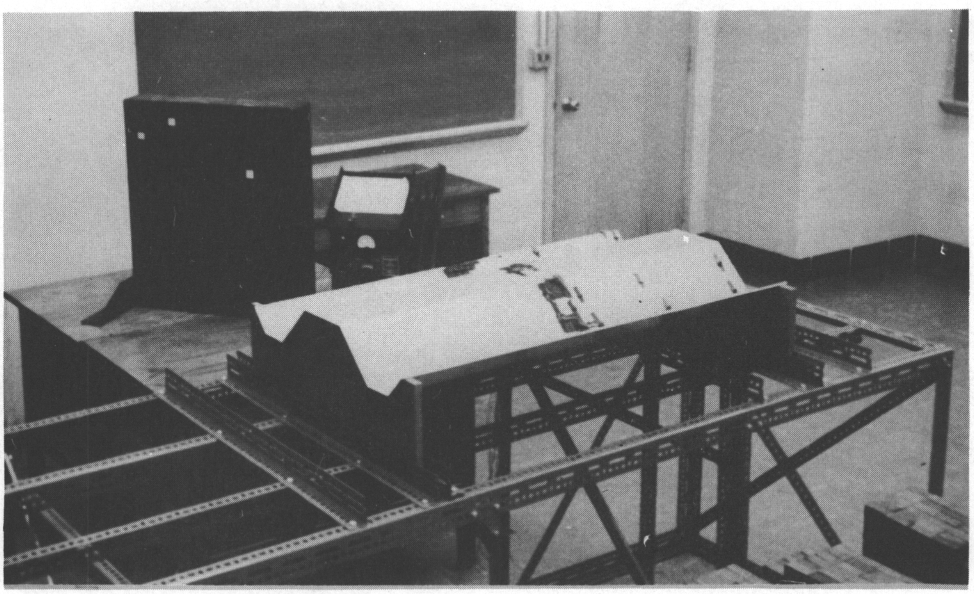

FIGURE 10. MODEL 2

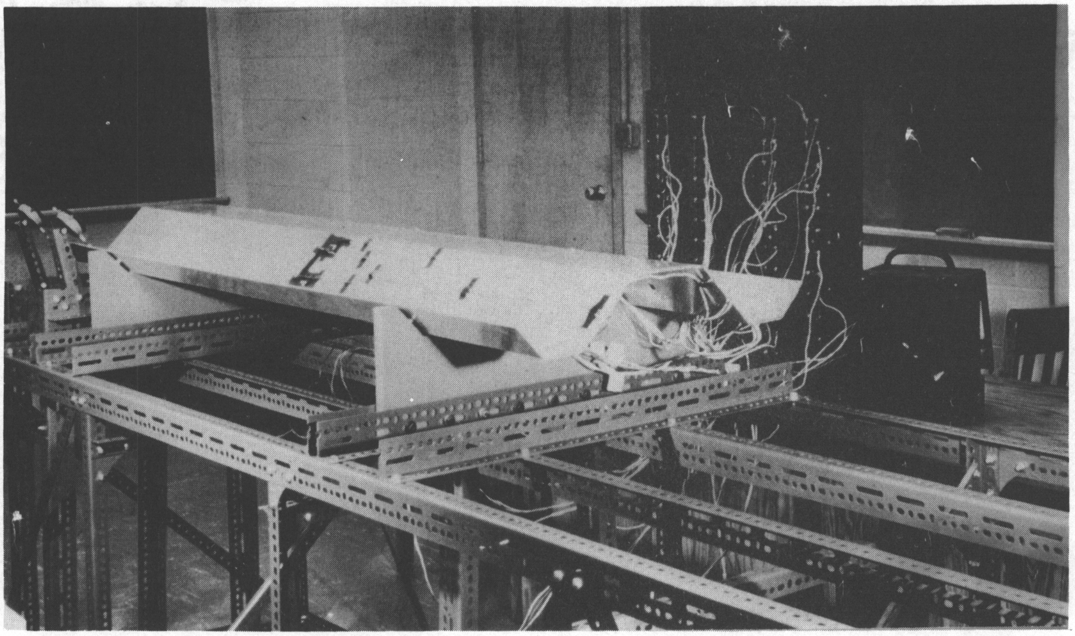

FIGURE 11. MODEL 3

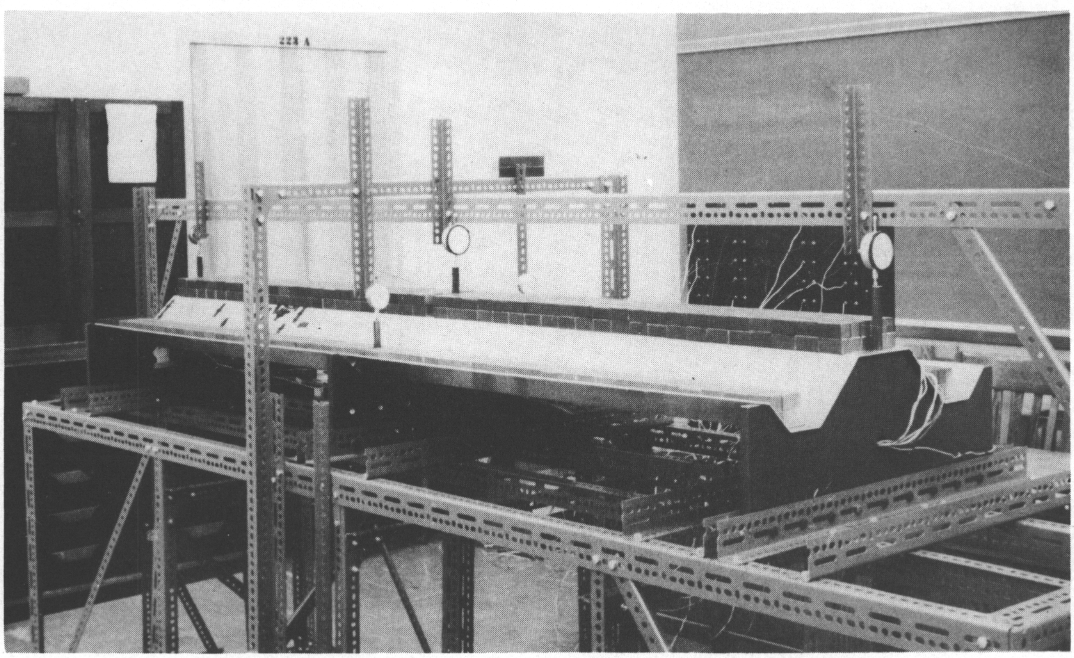

FIGURE 12. MODEL 4

results would indicate the degree of reliability to be expected from the experimental investigation.

The other three models consisted of seven plate surfaces: Model 2 (Figure 10) was a simply supported, single-span structure; Model 3 (Figure 11) was a single-span structure with overhangs at each end; Model 4 (Figure 12) was a two-span, continuous structure with simply supported end conditions. Model 2 was tested to establish experimental verification of the general method of analysis of the simply supported, single-span folded plate surface. Model 3 and 4 were used to establish the necessary experimental verification of the behavior of the continuous folded plate surface as predicted by the proposed general method of analysis.

The hipped-plate form of folded plate surface with horizontal plates at the ridges and valleys was chosen for the model study in preference to the V-shape with all sloping plates primarily in order to simplify the loading process and to assure uniform distribution of the applied load.

B. DESCRIPTION OF MODELS

The models were constructed of 1100-H14 sheet aluminum, 0.090 inches thick. The material was chosen for its strength, workability and capability of providing a desirable test strain range for reasonable length to width to thickness ratios. This material has a modulus of elasticity of 10.6×10^6 psi and a Poisson's ratio of 0.33. (These constants are the manufacturer's recommended values and were verified by a simple tension test on a 1.0" x 0.09" x 9.0" coupon of the material). In order to establish continuity at the fold lines, each surface was formed from individual sheets cut from commercially available sizes by shearing and bent on a sheet metal brake. The supporting diaphragms were wood cut from 12" x 1" pieces of fur and fastened to the folded plate surface with wood screws.

The dimensions of the models (Figure 13) were selected using a scale factor of approximately 1/20 of a typical prototype reinforced concrete folded plate surface. The thickness was further reduced by a factor of approximately two to account for the difference in moduli of elasticity of concrete and aluminum and to increase the flexibility of the model.

During the testing, the models were placed on a supporting frame (Figure 12) constructed of "Dexion" (slotted angles of light gage steel). Each supporting diaphragm was connected by bolts to a horizontal pair of angles, one on either side of the diaphragm, which in turn were connected to the framework. The supporting angles were torsionally flexible and offered essentially no restraint to the simple support action; the connections between the surface and diaphragms did not restrain the plates against rotation.

The models were instrumented with SR-4, A7 strain gages to record longitudinal and transverse strains at selected points on the surface. These were arranged in pairs in a tee pattern with one pair on the top face and another pair at the same point on the

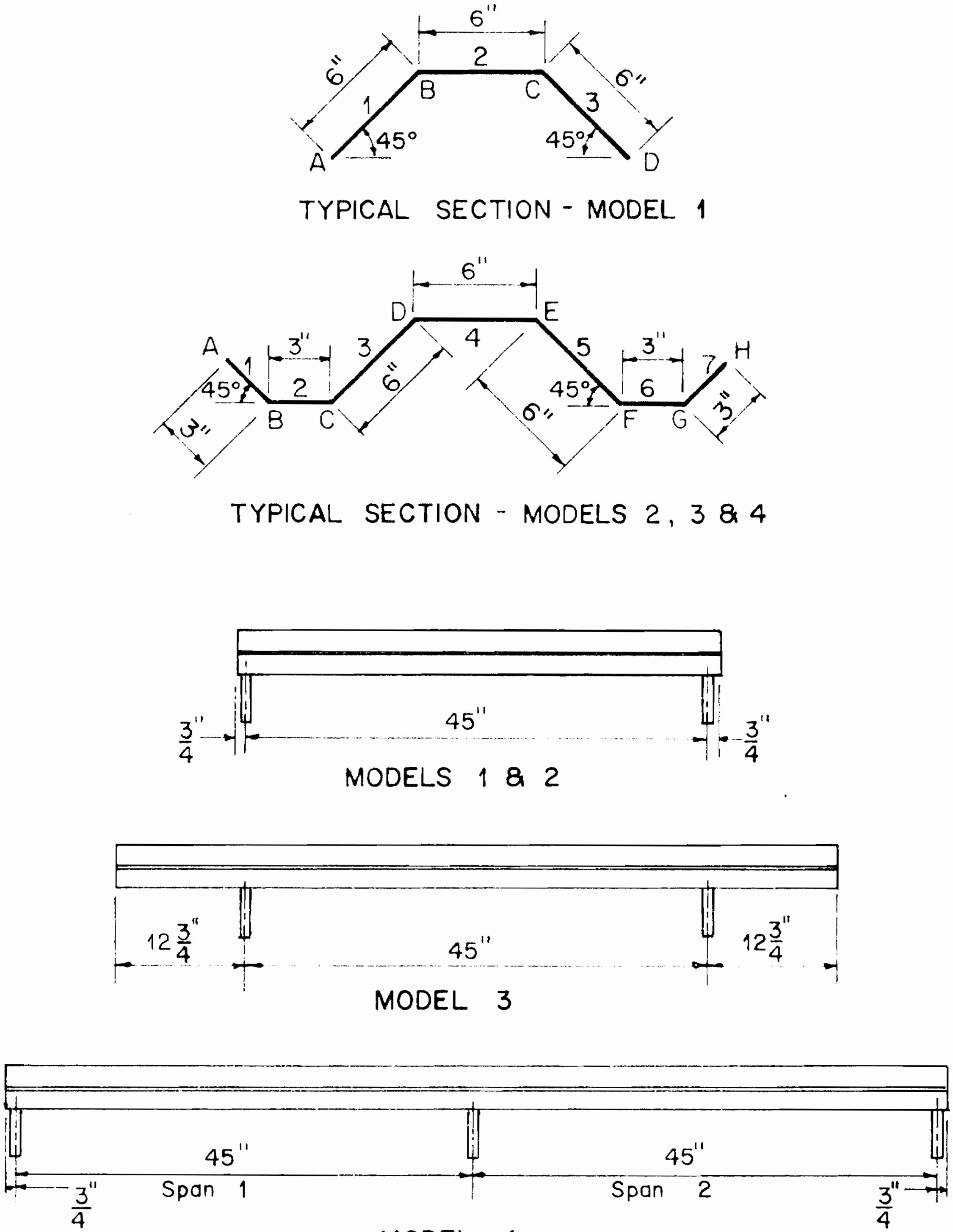

FIGURE 13. DETAILS OF MODELS

bottom face. One gage of each pair was oriented to measure the longitudinal strains and the other was oriented to measure the transverse strains. The location of the strain gages on the surface of each model is shown in Figures 14, 15 and 16.

C. TEST PROCEDURE

For the experimental investigation, each structure was studied under the action of uniform load superimposed on the horizontal plates of the surface (Figure 12). The loading was applied by stacking steel blocks, approximately 1" x 1" x 2", over the surface of the horizontal plates in a series of layers, each layer producing an incremental surface load of 40.26 psf. Strain readings were taken for each increment of loading and unloading of each structure.

For Models 1, 2 and 3, two complete sets of readings were taken in cyclic order for each increment of surface load. The final reading for each gage was established by averaging. It was found that for the usual time interval of about ten minutes between the first and second reading of each gage, the second reading was approximately ten micro-inches per inch less than the first regardless of whether the strain was positive or negative. This phenomenon was believed to be peculiar to the electrical strain measuring equipment which was used rather than being caused by creep of the structure. The ten micro-inch per inch decrease was fairly consistent regardless of the level of strain or the amount

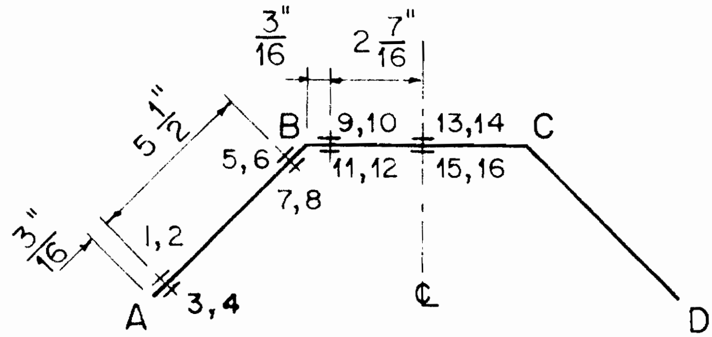

MODEL 1 - SECTION AT MIDSPAN

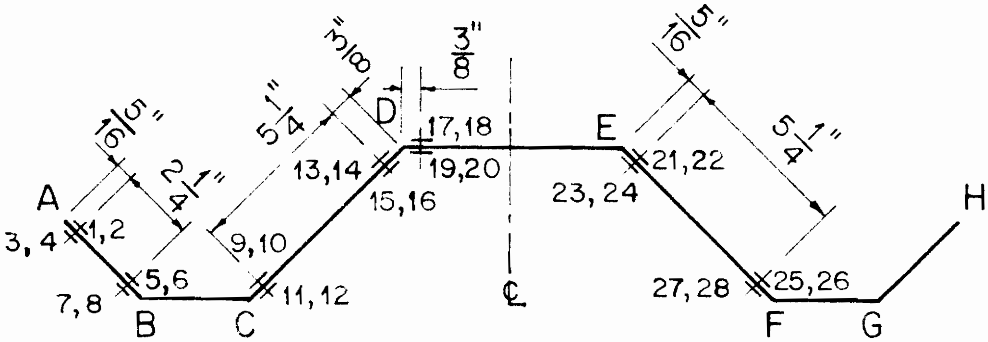

MODEL 2 - SECTION AT MIDSPAN

Odd numbered gages – longitudinal direction

Even numbered gages – transverse direction

FIGURE 14. LOCATION OF STRAIN GAGES — MODELS 1 AND 2

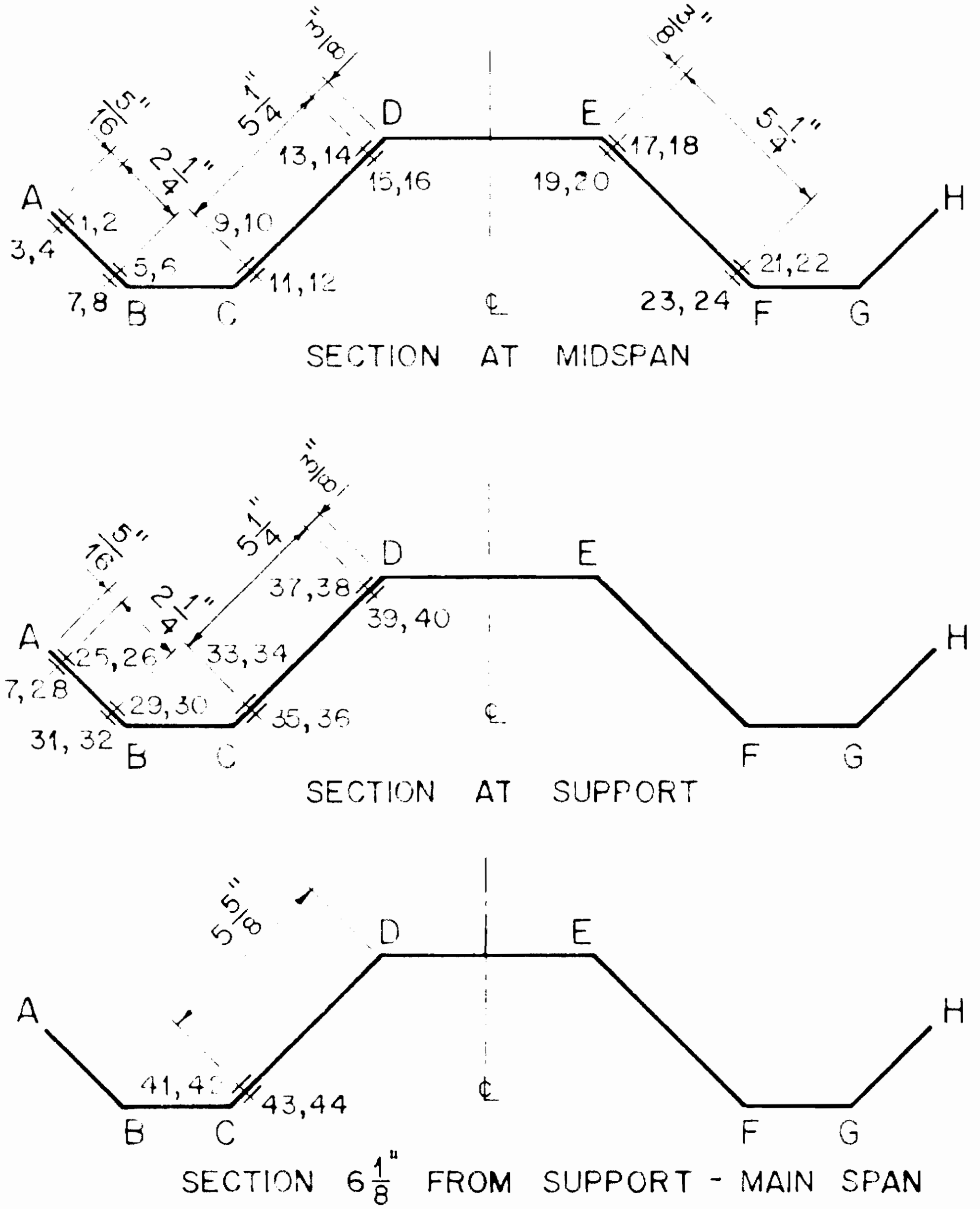

Odd numbered gages – longitudinal direction
Even numbered gages – transverse direction

FIGURE 15. LOCATION OF STRAIN GAGES - MODEL 3

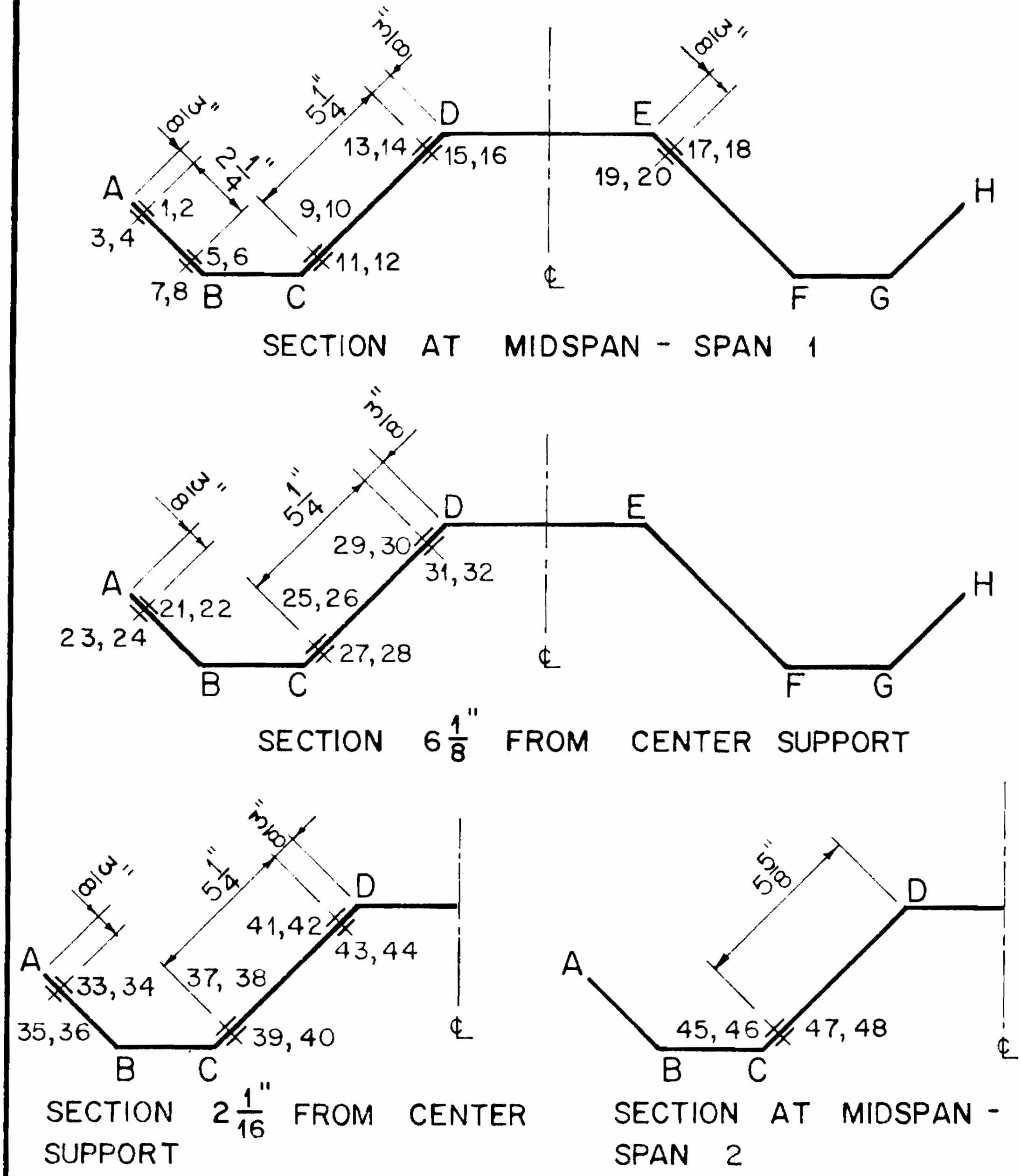

Odd numbered gages – longitudinal direction
Even numbered gages – transverse direction

FIGURE 16. LOCATION OF STRAIN GAGES - MODEL 4

of strain; when several additional cycles of readings were made, there were essentially no further differences noted.

Each model was loaded and unloaded several times with three to five increments of 40.26 psf each. The strains were calculated for each increment of load and the average of at least 18 readings were used in the analysis. The average strains determined for each gage on each model are listed in Appendix C.

Dial gages were placed at selected points and were used primarily as a means of control and verification of structural action during the testing of the structures. During the course of testing, the supporting diaphragms were found to settle as the structures were loaded. Two factors contributed to this settlement; (1) the compressibility of the wood and (2) the flexibility of the supporting light gage steel framework. The settlement of supports of the single-span structures did not affect the internal stresses but intermediate deflection measurements had to be corrected for support settlement. For the two-span structure, however, any movement of one support relative to the other two supports did cause additional internal stresses to be developed in the surface. In order to compensate for this relative movement of supports, the center support was adjusted by jacking after the application of each increment of loading to maintain its alignment with the end supports. The jacking system used for the procedure is shown in Figure 17.

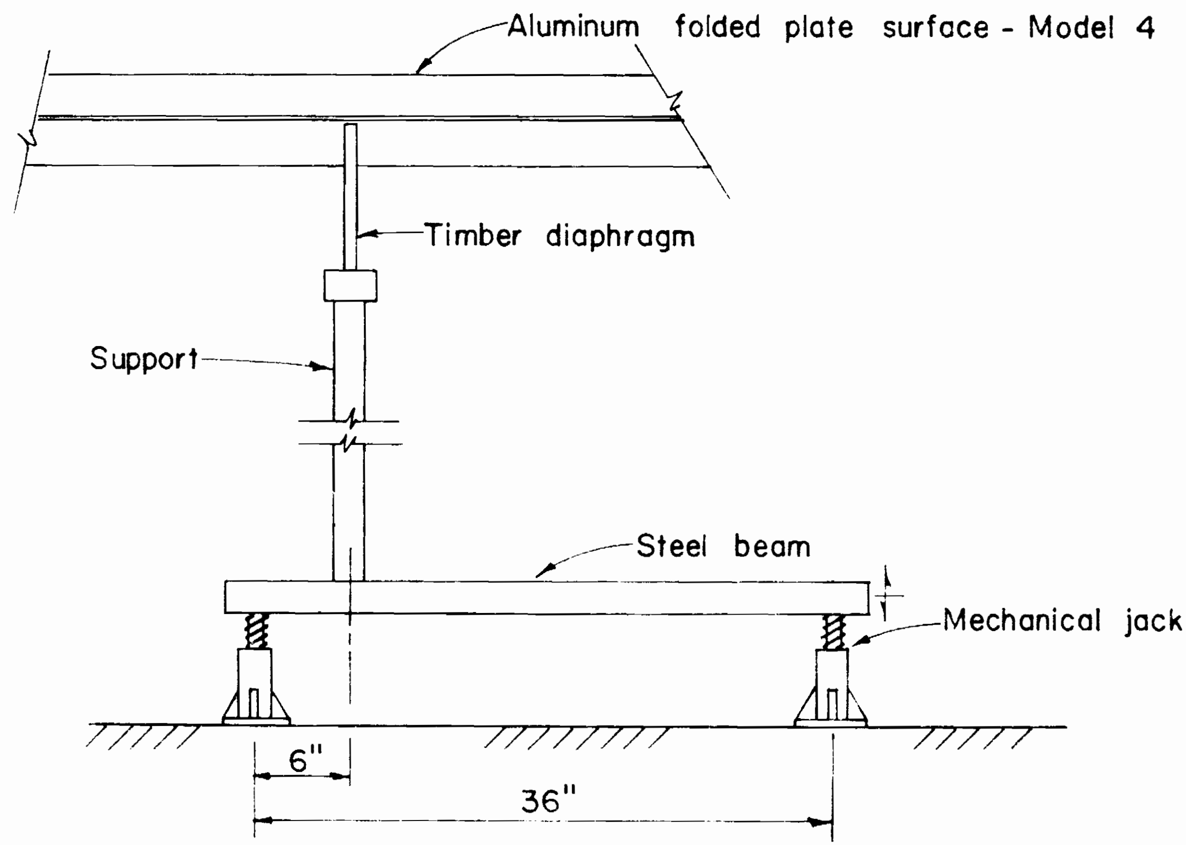

FIGURE 17. JACKING SYSTEM — MODEL 4

D. COMPARISON OF EXPERIMENTAL AND THEORETICAL ANALYSIS

The comparison of experimental and theoretical values of longitudinal stresses and transverse moments developed in the surfaces of the four models is presented in Figures 18 through 23. The distribution of longitudinal stresses and transverse moments across the sections was established from the theoretical analysis. The experimental values are those given in parenthesis. Also, in Appendix C, a comparison is made between the experimental strains and the theoretically predicted strains.

The theoretical values for longitudinal stress and transverse moment for Models 2, 3 and 4 were obtained from the solution of the action of the folded plate surfaces by the general method of analysis presented in Section IV using the IBM 1620-60k electronic computer. For Model 1, which was a statically determinate folded plate surface (three plates), the theoretical values were calculated by hand, using the technique of analysis presented by Simpson[8] for a "membrane" analysis alone.

The stresses occurring in the surfaces at the different gage locations for the applied loading were computed using the familiar relationships of elasticity:

$$f_1 = \frac{E}{1 - \mu^2} (\epsilon_1 + \epsilon_t)$$

$$f_t = \frac{E}{1 - \mu^2} (\epsilon_t + \epsilon_1)$$

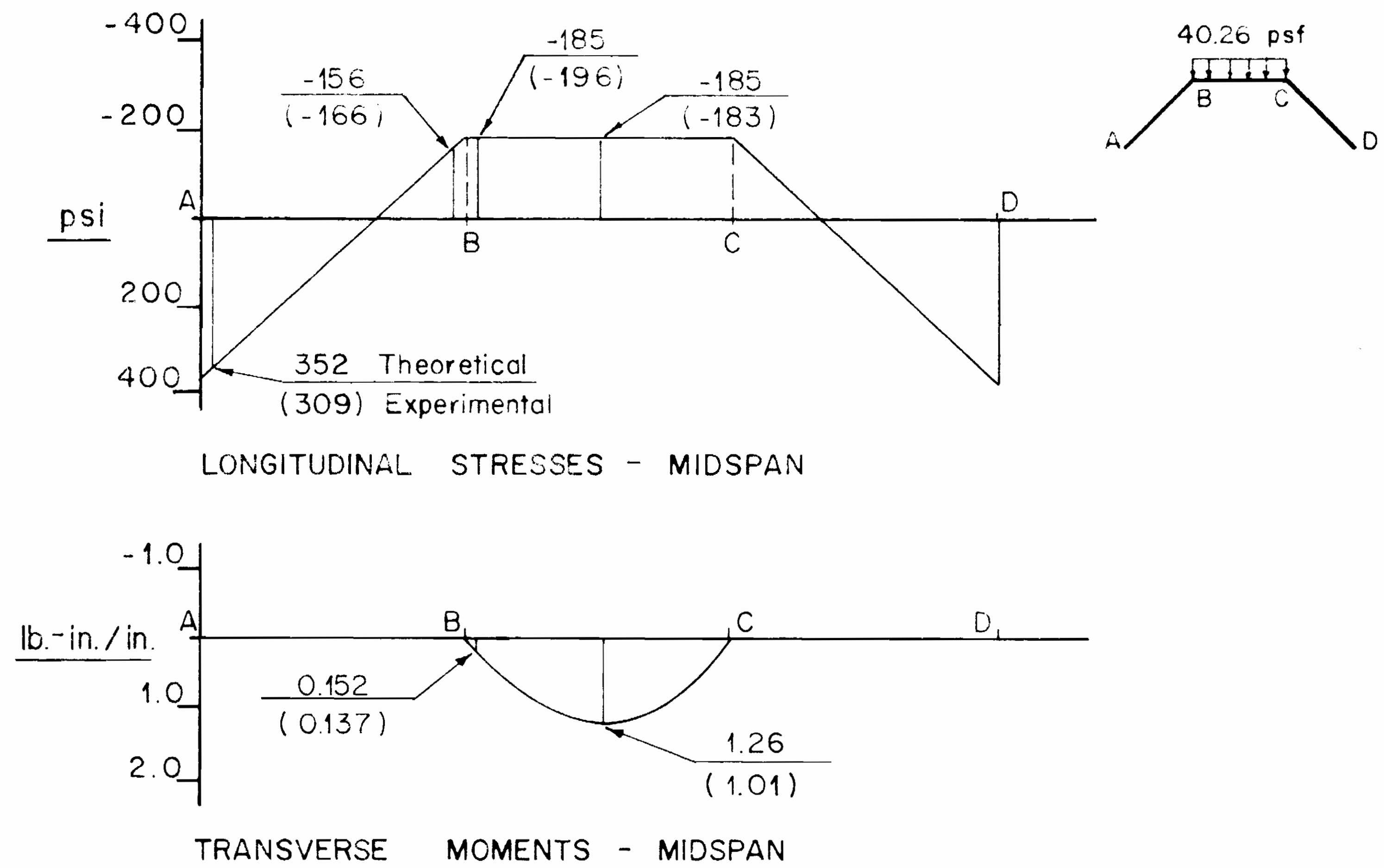

FIGURE 18. MODEL 1 - VALUES OF STRESSES AND MOMENTS

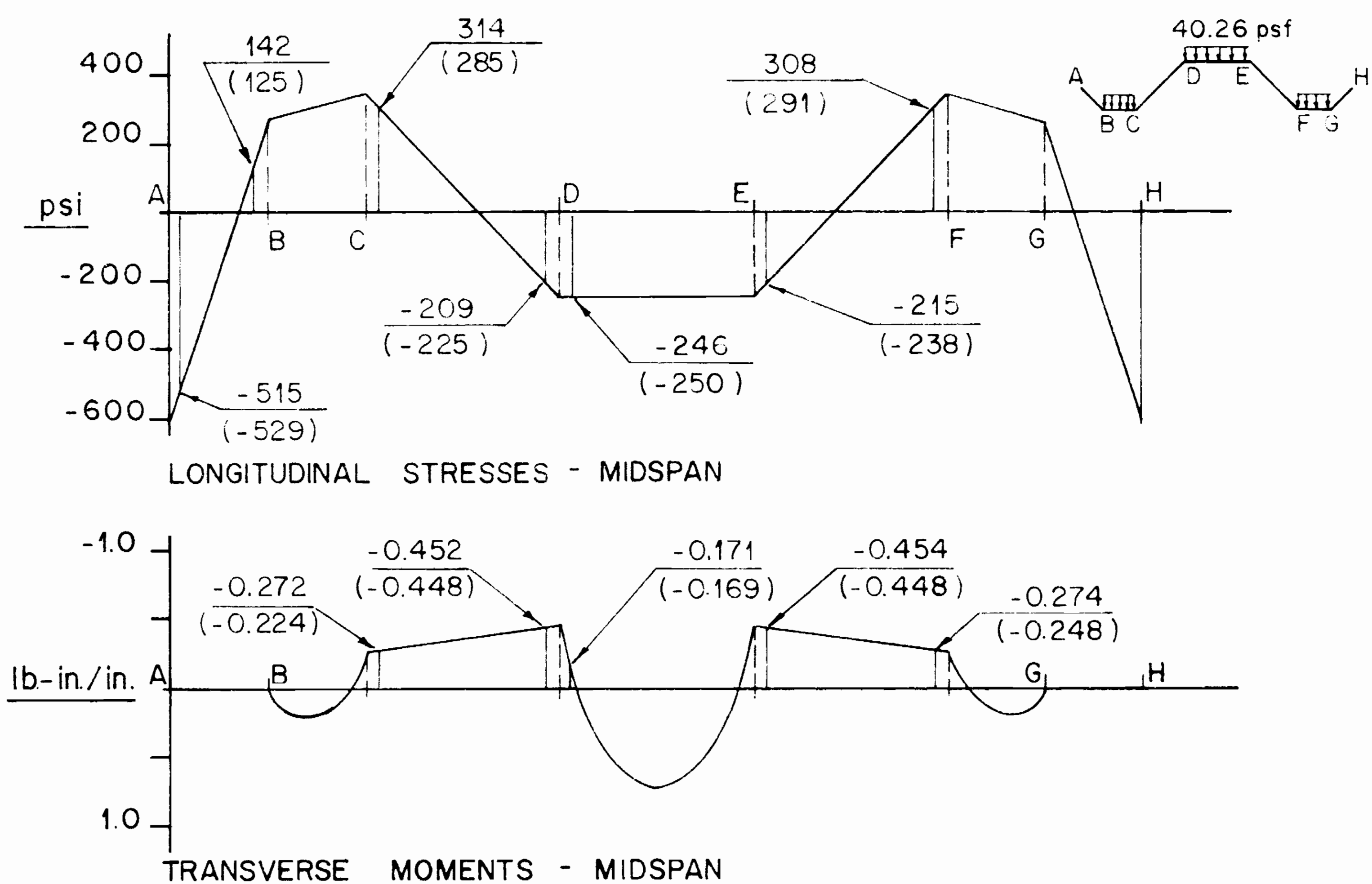

FIGURE 19. MODEL 2 - VALUES OF STRESSES AND MOMENTS

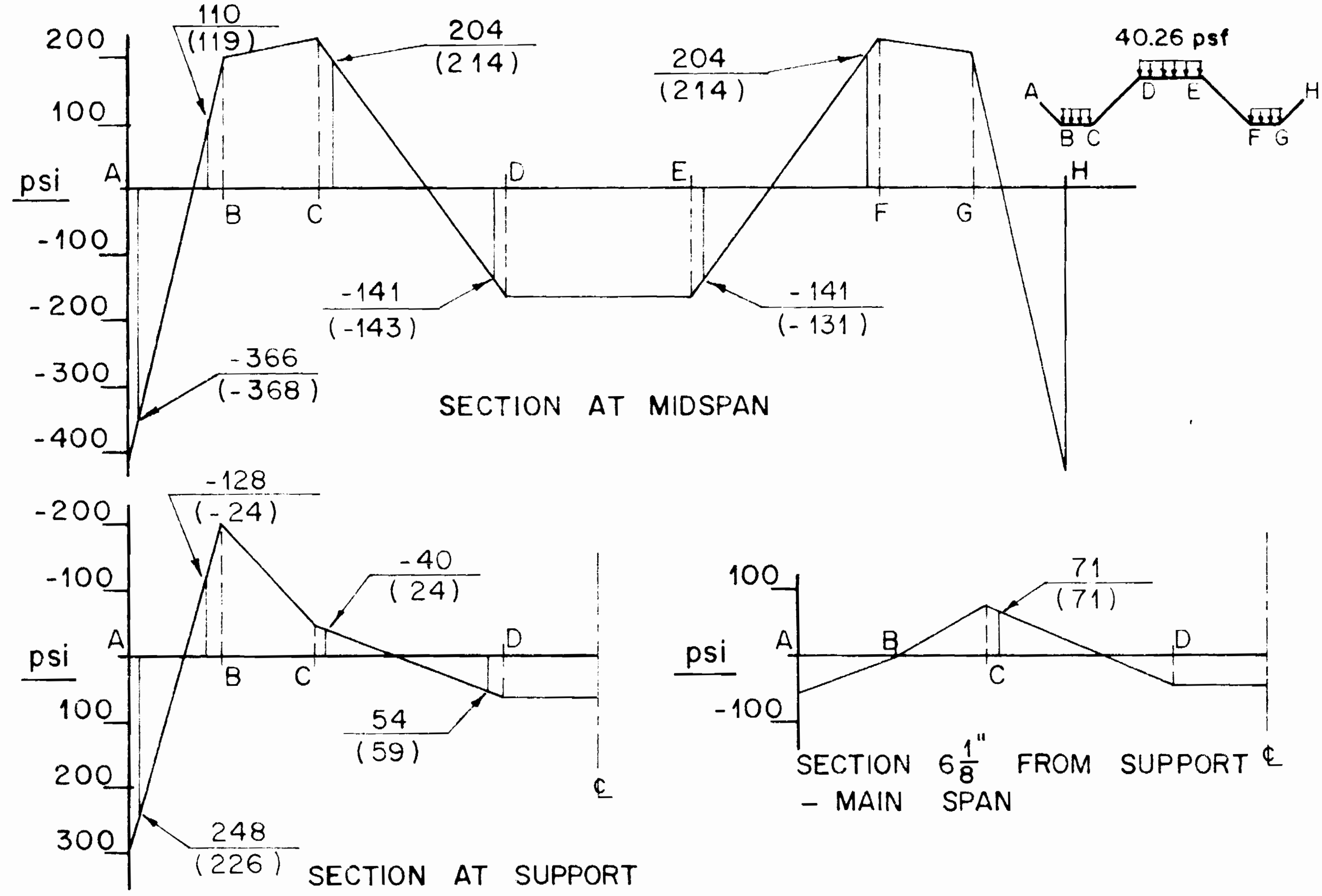

FIGURE 20. MODEL 3 – LONGITUDINAL STRESSES

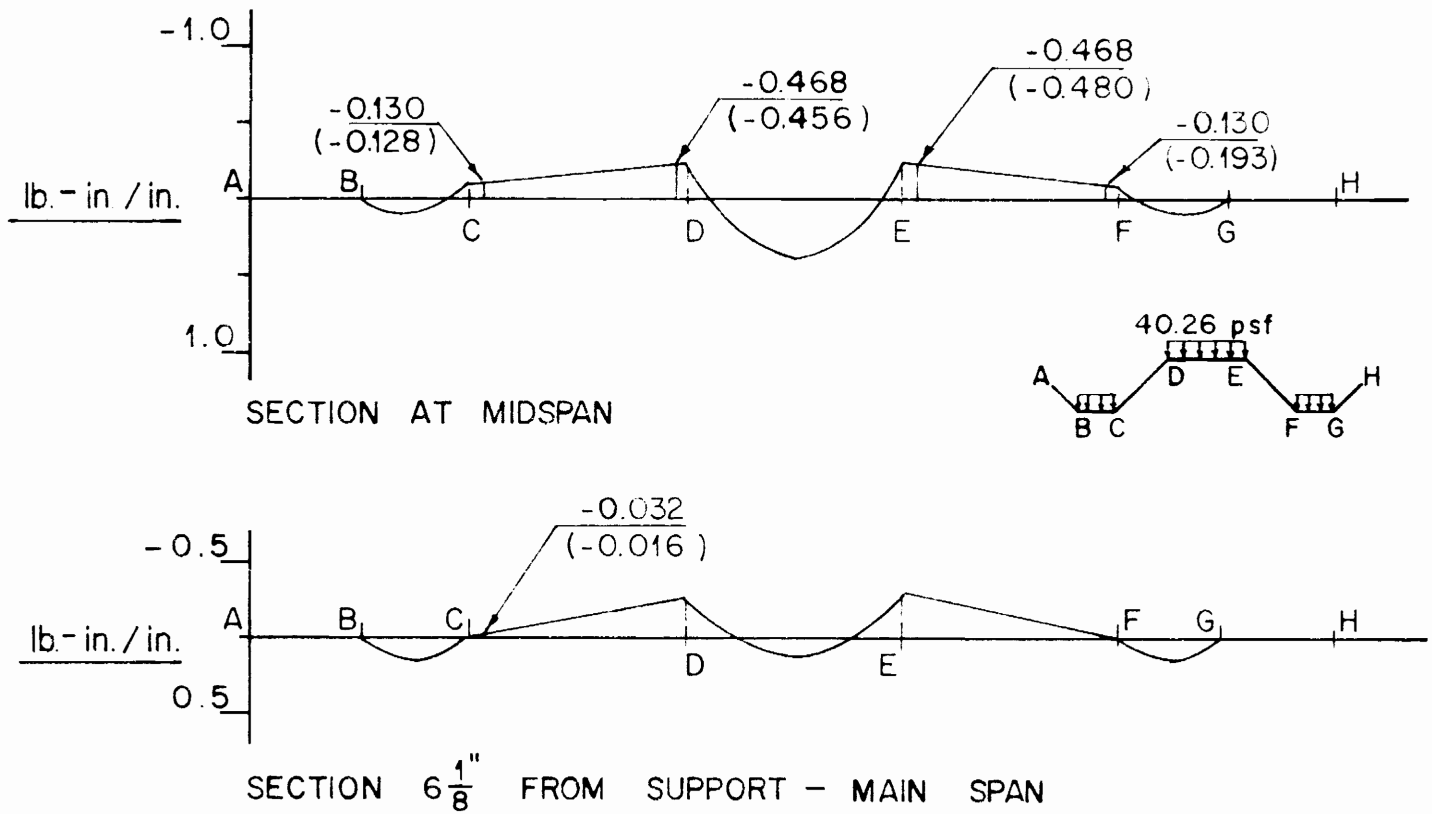

FIGURE 21. MODEL 3 - TRANSVERSE MOMENTS

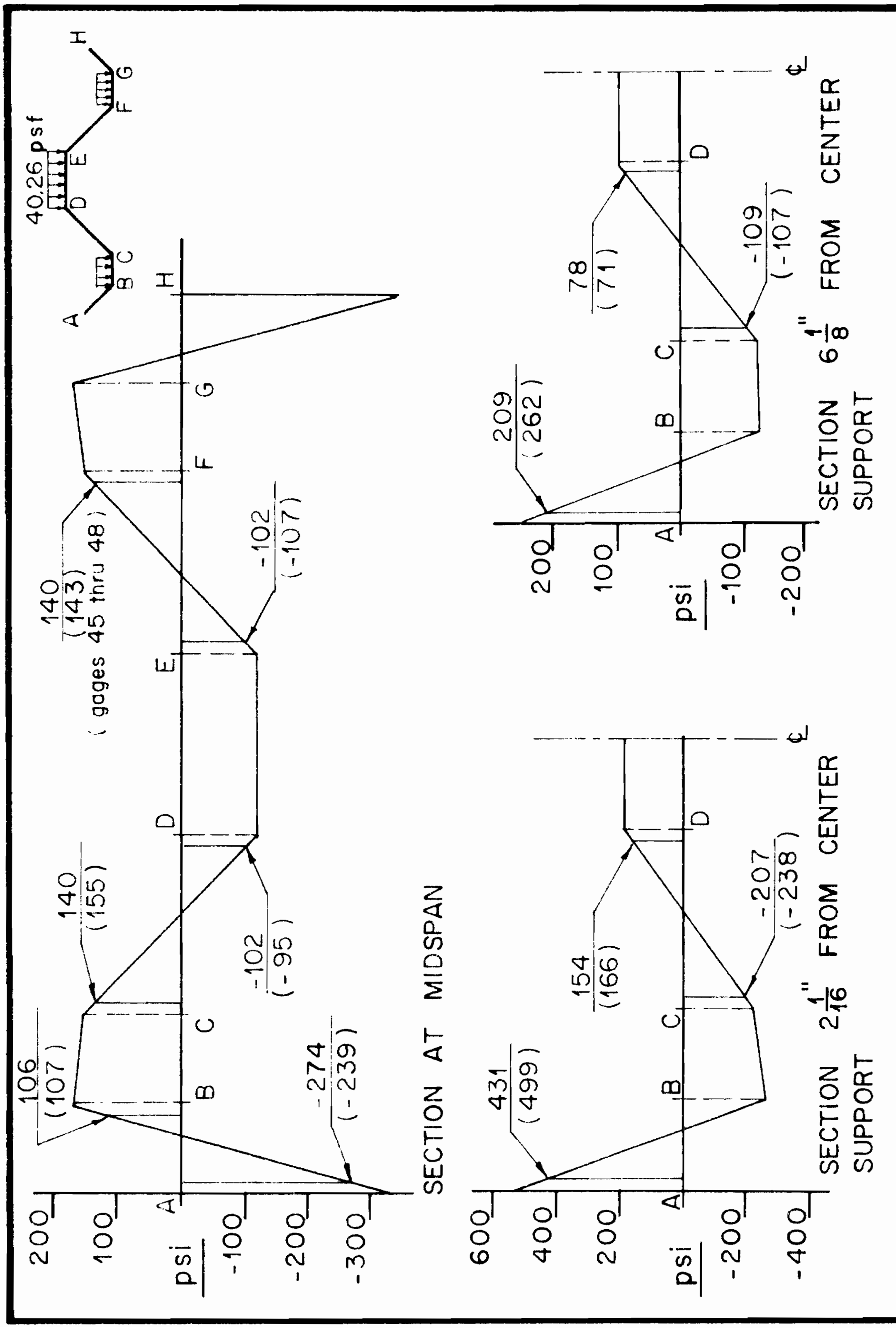

FIGURE 22. MODEL 4 — LONGITUDINAL STRESSES

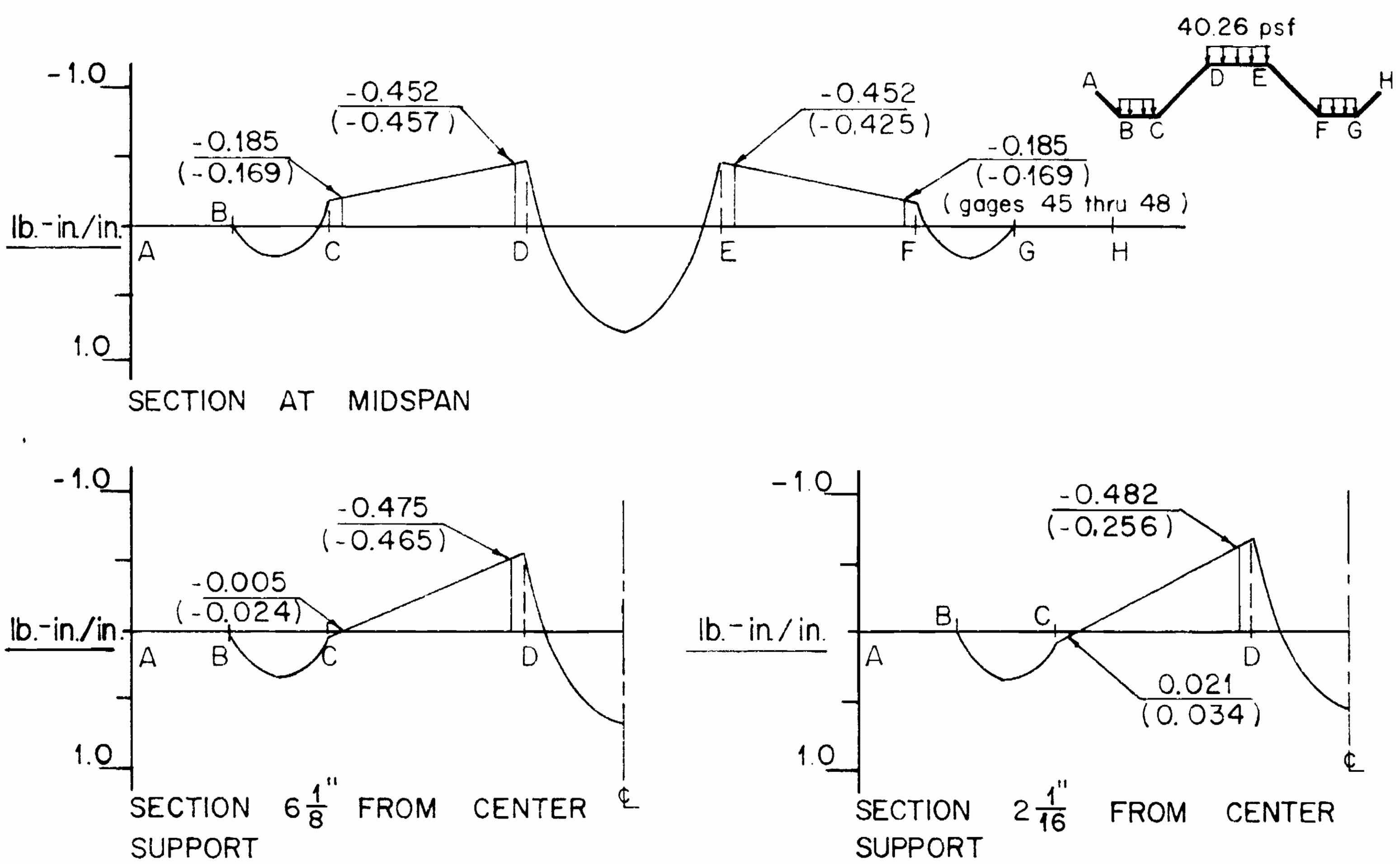

FIGURE 23. MODEL 4 — TRANSVERSE MOMENTS

where ϵ_l = average longitudinal strain, in./in.

ϵ_t = average transverse strain, in./in.

f_l = longitudinal stress, psi

f_t = transverse stress, psi

E = modulus of elasticity, 10.6 x 10^6, psi

μ = Poisson's ratio, 0.33 .

The stresses were calculated for both the longitudinal and transverse directions for each of the pairs of gages on the top and bottom faces (Appendix C). The experimental values of the longitudinal stress resulting from the beam action of the individual plates were found by taking an average of the values of longitudinal stress at the top and bottom faces, eliminating the effects of longitudinal slab bending. The values of transverse stress resulting from the transverse bending were established by taking an average of the difference of the transverse stress at the top and bottom faces, eliminating the effects of any transverse axial stress.

An examination of the experimental and theoretical results obtained for the four models (Figures 18 through 23; Appendix C), in general, reveals very good agreement and substantiates the use of the general method of analysis to establish the behavior of simply supported, single-span or continuous-span folded plate surfaces.

With the exception of the values of transverse moments at the midspan of Model 1, excellent agreement between the experimental and theoretical values for Models 1 and 2 (Figures 18 and 19) was obtained and thus established the reliability of the experimental investigation. During the testing of Model 1, the load was not applied quite uniformly over the surface of the horizontal plate in the vicinity of the gages although the total load was equivalent to 40.26 psf over the entire horizontal surface. To prevent the placement of the steel blocks directly on the gages, small platforms were located around the gages and the blocks were supported on these. This discontinuity of loading in the vicinity of the gages may account in part for discrepancy in the values of transverse moments at the midspan of Model 1.

In Model 3, the surface with overhangs at the ends, it was noted that there was an unusually large discrepancy in the longitudinal stresses from that predicted at the section at the line of support. The strain measurements were verified by repeated loading and unloading, and it was concluded that the discrepancy was caused by local effects of the supporting diaphragm. In order to facilitate the placement of strain gages over the line of support, the diaphragms were cut away from the inclined plates (plates 1, 3, 5 and 7). The plates were then supported on small washers placed on the connecting screws between the plates and the diaphragms. Plates 1 and 7 were supported at each diaphragm at just one point, in the center of the plates, and plates 3 and 5 were supported at each diaphragm at two points, approximately one inch from each fold line. An examination of the strains, listed in Appendix C, recorded by gages at the support (gages 25 through 40) shows the development of transverse bending moments. These moments could not have occurred had the plates been supported along their entire width by the supporting diaphragm. Also, some longitudinal bending moment was developed by the longitudinal slab action of the plates which is neglected in the general method of analysis.

For Model 4, the comparison of the experimental and theoretical values of transverse bending moments (Figure 23) shows good agreement. For the most part, any difference noted con be accounted for by the fact that relatively small strain increments were being measured and the tolerance of the measuring equipment used was dependent upon the magnitude of strain. The only difference that might be of concern is at the section two and one-sixteenth inches from the center support (Figure 23) of Model 4, plate 3 (gages 41, 42, 43 and 44) where the experimental value is approximately 50% of the theoretical value. The theoretical value of transverse moment at this point has been determined assuming only one-way slab action of the plates, and thus neglecting the influence of the supporting diaphragms on the longitudinal distribution of the transverse moments. Since the support diaphragms were rigid in their planes, two-way slab action occurred in the vicinity of the supports, resulting in longitudinal slab action over the supports and zero transverse moments in the line of supports. Because of the two-way slab action near the supports, the magnitude of the transverse moments are reduced, as indicated by the experimental value. It should be pointed out that at the section six and one-eight inches from the center support there was very good agreement between the theoretical and experimental values. This indicates that the influence of the two-way slab action of the longitudinal distribution of transverse moment does not extend beyond a distance of approximately one half the width of the plate on either side of the support. In the design of a folded plate surface this effect near the supports should not be overlooked.

E. DISCUSSION OF RESULTS

The results of this investigation have confirmed the application of the general method of analysis presented in Section IV for defining the behavior of the folded plate surface. This was demonstrated by the excellent agreement between the experimental and theoretical values of longitudinal stress and transverse moment (Figures 18 through 23) for all four models. An examination of the data presented in Appendix C and Figures 18 through 23 shows that the experimental values agree with the theoretical values with differences of from 0 to 5% in about 40% of the cases, 5 to 10% in about 30% of the cases and 10 to 15% in about 11% of the cases. There were a few isolated cases where the differences were higher than 20% but these have been accounted for and discussed in Section VI-D and in the following paragraphs. With the test set-up that was used and the magnitude of strain-increment measurements that were made, agreement between experimental and theoretical values within 10 to 15% would be considered acceptable.

Also to be noted in Appendix C is the relatively small magnitude of strains that were being recorded. The strain indicator was marked in intervals of ten micro-inches per inch; readings were estimated to the nearest one micro-inch per inch. Normal reliability of the equipment allows for variations of $\pm$ 5 to 10 micro-inches per inch. Working with small strains, a variation of only one or two micro-inches per inch could have had a rather large effect on the relative agreement between the experimental and theoretical values of stress. This problem was anticipated so extreme care was taken to make very careful readings and to develop a consistent routine in taking the readings to avoid extraneous variations. It should be mentioned that plaster and plastic were considered as possible materials for construction of the models but aluminum sheet was chosen because it was not fragile nor subject to excessive creep at low stresses. Thinner sheet aluminum would have assured larger strain readings but would have introduced the possibility of buckling. Larger loads could have been applied but this was found not to be practical for the laboratory facilities available.

Besides the errors due to the equipment that was used, errors could have been introduced by variation in temperature and humidity in the laboratory which would cause non-uniform variation in the strain readings. Temperature and humidity were noted and care was taken to avoid variations. Minor variations would have been cancelled out over the many repetitions of loading and unloading of the models.

An additional source of error was noted in the test of

Model 4. There were unequal deflections of the supports during loading. With each increment of loading of the surface (40.26 psf), the center support was found to deflect about 0.009 inches more than the end supports. This appeared to be due to compression of the wood diaphragms and the flexibility of the supporting framework under load. It should be pointed out that the center support carried about $2\frac{1}{2}$ times as much load as the end supports. Although this movement represented a total span deflection of only L/5000 (where L is the span length), there were some very large stresses introduced in the surface. In the vicinity of the center support this movement was sufficient to cause, in some cases, a reversal in stresses. In order to compensate for this relative movement, the center support was jacked into alignment with the end supports after the application of each load increment. The jacking system used for this operation is illustrated in Figure 17. With dial gages located at the center of each support, the movement of the support in the jacking operation could be controlled to the nearest 0.0005 inches.

Although the models were well constructed and quite accurate there was some noticeable initial deviation from the prescribed deflection angles (a_j) along some of the fold lines. The manufacturer was able to correct most of this deviation by additional passes through the brake, and some was removed when the surfaces were connected to the diaphragms. Although the plate dimensions were fairly accurate, the variation in the deflection angles between the adjacent plates was as much as 4° from the prescribed 45°; there was also some slight variation in the deflection angles in the longitudinal direction. A theoretical study of the effect of this variation in the deflection angles was made for Model 2 and the results indicated a difference of 3 to 4% in the final solution of stresses and moments for a 2° variation in the deflection angles between the plates.

The location of the strain gages were determined by measurement from the fold lines of the surfaces. Since the surfaces were made from individual sheets bent to shape, there were no well defined edges to use as a reference in locating the gages on each plate. The positions may be considered as noted in Figures 14, 15 and 16 within ± approximately 1/32 inches. An error of 1/32 inches would result in an error of up to 3% in determining theoretical stresses.

VII ILLUSTRATIVE EXAMPLES

To illustrate the application of the general method of analysis of the folded plate surface and the computer program utilizing the IBM 1620-60k electronic digital computer, two illustrative examples are presented.

In Example 1 (Figure 24), a simply supported, single-span, reinforced concrete folded plate surface is analyzed for a dead load of 80 psf (load condition (2) as described for the computer program, Section V). This example is the same as that presented as an illustrated example by H. Gesund[18]. The presentation of this example permits the comparison of a solution obtained by the general method of analysis presented here with one obtained by the presently accepted method of analysis for the single-span, simply supported folded plate surface as presented by Gesund. The results obtained by the general analysis, as well as the results determined by Gesund, are listed in Table 1. The values of the two solutions at midspan are the same and only small differences of up to approximately 6% occur between the exact longitudinal distribution of the moments and forces as established by the general method of analysis and the sinusoidal distribution as assumed by Gesund (Figure 25). The longitudinal distribution of the transverse moments along the fold lines has been rather vague as presented in previous literature. However, as a result of the general analysis, it will be noted that the value of the transverse moments along a

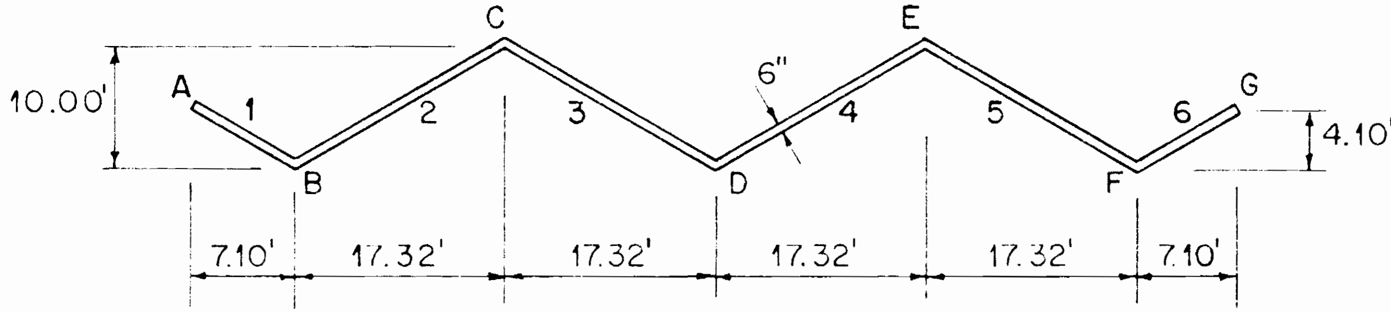

Dead Load:		
	Concrete	75 psf
	Roofing	5 psf
	Total	80 psf

a) TRANSVERSE SECTION

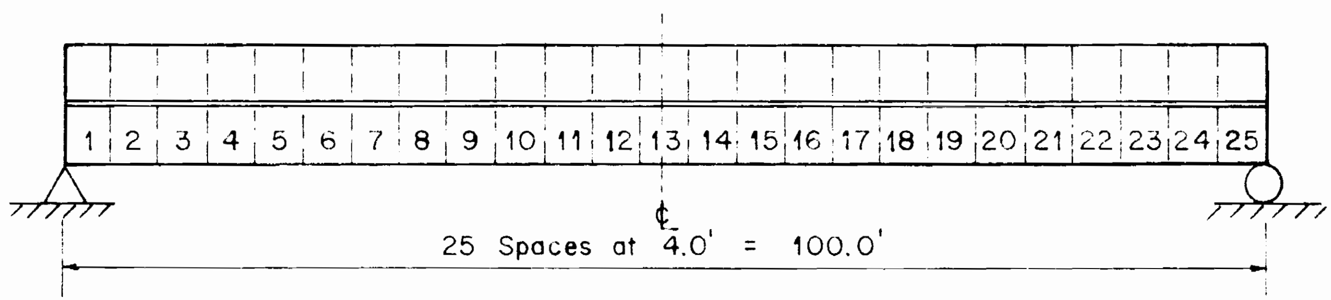

b) LONGITUDINAL SPAN

FIGURE 24. EXAMPLE 1

TABLE 1 EXAMPLE 1 - FINAL SOLUTION

Segment	TRANSVERSE MOMENTS (TM''_{jm}) ft-k			EDGE SHEAR FORCES (N''_{jm}) kips			LONGITUDINAL MOMENTS (LM''_{im}) ft-k			Segment
	Fold Line			Fold Line			Plate			
	B	C	D	B	C	D	1	2	3	
1	-2.33	-2.42	-2.27	11.6	- 2.8	0.0	- 91	403	- 345	25
2	-2.33	-2.65	-2.18	32.8	- 8.0	0.0	- 259	1143	- 981	24
3	-2.33	-2.87	-2.09	52.0	-12.7	0.0	- 413	1819	-1516	23
4	-2.33	-3.08	-2.01	69.3	-17.1	0.0	- 552	2430	-2086	22
5	-2.33	-3.28	-1.93	84.6	-20.9	0.0	- 675	2977	-2555	21
6	-2.33	-3.46	-1.86	98.1	-24.4	0.0	- 784	3459	-2969	20
7	-2.33	-3.62	-1.80	109.8	-27.4	0.0	- 879	3877	-3328	19
8	-2.33	-3.76	-1.75	119.6	-29.9	0.0	- 958	4230	-3632	18
9	-2.33	-3.88	-1.70	127.6	-32.0	0.0	-1023	4519	-3880	17
10	-2.33	-3.98	-1.66	133.8	-33.6	0.0	-1074	4744	-4074	16
11	-2.33	-4.04	-1.64	138.2	-34.8	0.0	-1110	4904	-4212	15
12	-2.33	-4.09	-1.62	140.8	-35.5	0.0	-1132	5000	-4294	14
13	-2.33	-4.10	-1.62	141.7	-35.7	0.0	-1139	5032	-4322	13
Gesund's Solution										
℄	-2.31	-4.14	-1.64	140.0	-36.0	0.0	-1139	5006	-4310	℄

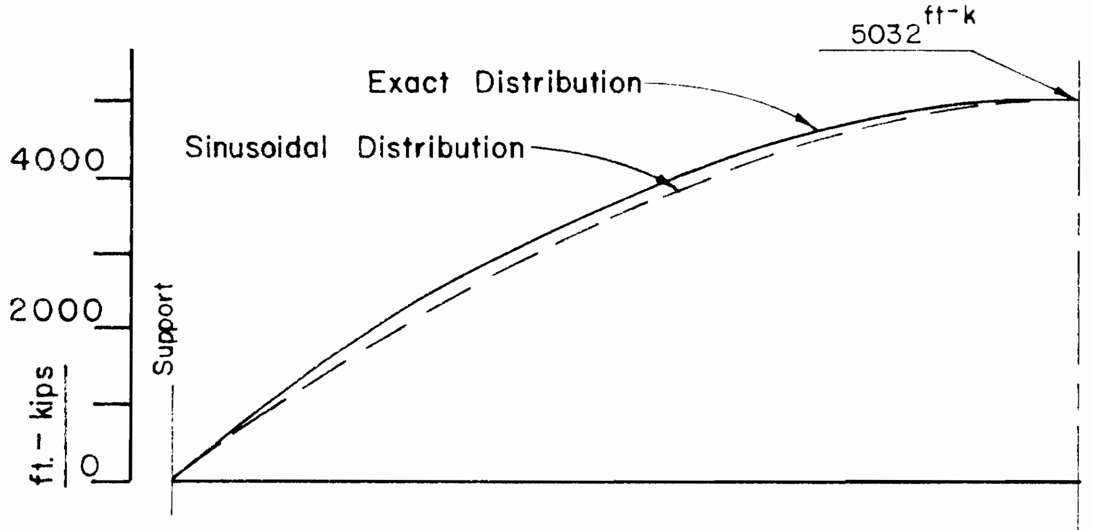

FIGURE 25. EXAMPLE 1 — LONGITUDINAL DISTRIBUTION OF LONGITUDINAL BENDING MOMENT (LM''_{im}) — PLATE 2

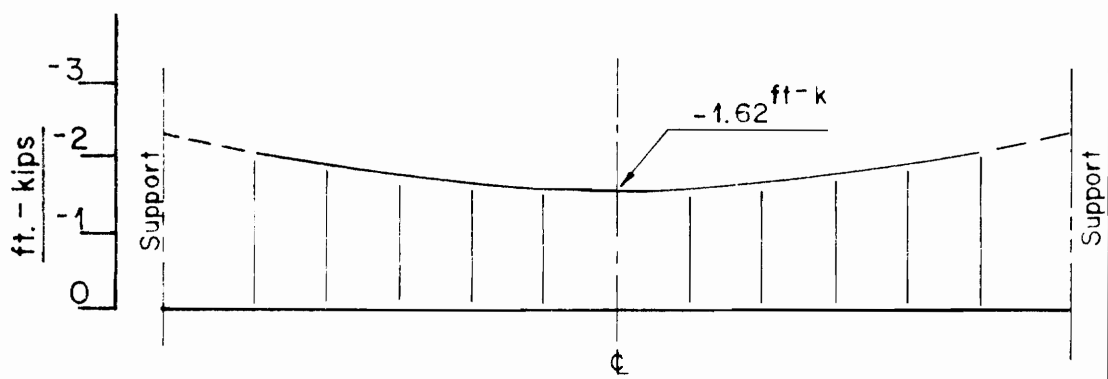

FIGURE 26. EXAMPLE 1 — LONGITUDINAL DISTRIBUTION OF TRANSVERSE BENDING MOMENT (TM''_{jm}) — FOLD LINE D

fold line is completely defined. It should be noted in the illustrated problem that the transverse moment is not necessarily maxiumu at the center as might be expected. Rather, due to the plate rotations, the maximum value of transverse moment along some fold lines is found to be near the ends of the longitudinal spans, as for example in the longitudinal distribution of the transverse moments along fold line D, (Table 1 and Figure 26). Since the general method of analysis is based upon the assumption of one-way slab action and of rigid supporting diaphragms, it becomes necessary to modify the longitudinal distribution of the transverse moments to account for the two-way slab action near the supports (Figure 26).

In Example 2 (Figure 27), a two-span, continuous folded plate surface is analyzed for uniform, vertical line loads applied at the valley edges. The results of the general analysis are listed in Tables 2 and 3; Figures 28 through 35 describe the general patern of distribution of the forces, moments and stresses in the surface.

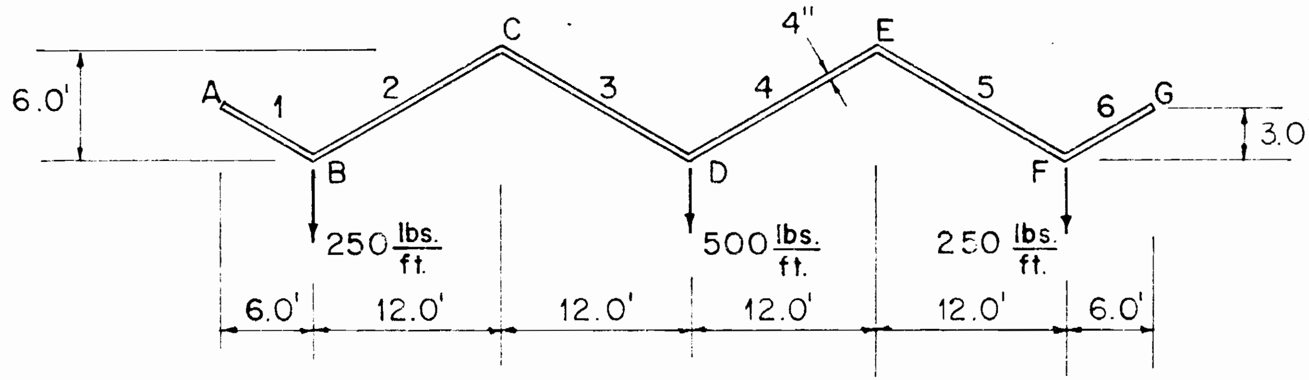

a) TRANSVERSE SECTION

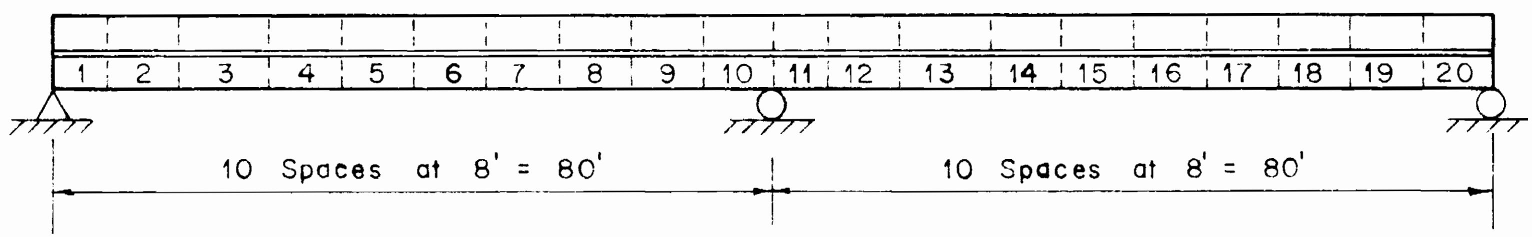

b) LONGITUDINAL SPAN

FIGURE 27. EXAMPLE 2

TABLE 2 EXAMPLE 2 - FINAL SOLUTION - TRANSVERSE MOMENTS AND EDGE SHEAR FORCES

Segment	TRANSVERSE MOMENTS (TM''_{jm}) ft-lb			EDGE SHEAR FORCES (N''_{jm}) kips			Segment
	Fold Line			Fold Line			
	B	C	D	B	C	D	
1	0.0	- 20	9	3.44	0.94	0.0	20
2	0.0	- 57	25	8.43	2.29	0.0	19
3	0.0	- 85	38	11.81	3.14	0.0	18
4	0.0	-102	45	12.91	3.50	0.0	17
5	0.0	-104	46	12.44	3.38	0.0	16
6	0.0	- 94	41	10.17	2.76	0.0	15
7	0.0	- 73	32	6.10	1.66	0.0	14
8	0.0	- 46	20	0.19	0.00	0.0	13
9	0.0	- 20	9	- 7.57	-2.06	0.0	12
10	0.0	- 12	1	-17.22	-4.68	0.0	11
Center Support				-23.00	-6.25	0.0	

TABLE 3 EXAMPLE 2 - FINAL SOLUTION - LONGITUDINAL MOMENTS, AXIAL PLATE FORCES AND LONGITUDINAL STRESSES

Segment	LONGITUDINAL MOMENTS (LM''_{im}) ft-k			AXIAL PLATE FORCES (P''_{im}) kips			LONGITUDINAL STRESSES (f''_{jm}) psi			
	Plate			Plate			Fold Line			
	1	2	3	1	2	3	A	B	C	D
1	- 21.2	63.9	- 60.4	- 3.4	2.5	0.9	- 70	48	- 40	43
2	- 52.2	157.5	-148.9	- 8.4	6.1	2.3	-171	119	-100	107
3	- 71.9	216.9	-205.1	-11.6	8.4	3.1	-236	164	-138	147
4	- 80.2	242.2	-229.1	-12.9	9.4	3.5	-263	183	-154	165
5	- 77.3	233.5	-220.8	-12.4	9.1	3.4	-253	176	-148	159
6	- 63.2	190.7	-180.3	-10.2	7.4	2.8	-207	144	-121	130
7	- 37.7	113.8	-107.5	- 6.1	4.4	1.7	-124	86	- 72	77
8	- 1.0	2.7	- 2.5	- 0.2	0.1	0.1	- 3	2	- 2	2
9	47.2	-142.5	134.7	7.6	- 5.5	-2.1	155	-108	90	- 97
10	106.7	-321.8	304.3	17.2	-12.5	-4.7	350	-243	204	-219
Center Support	142.2	-428.6	405.2	23.0	-16.8	-6.2	467	-324	272	-291

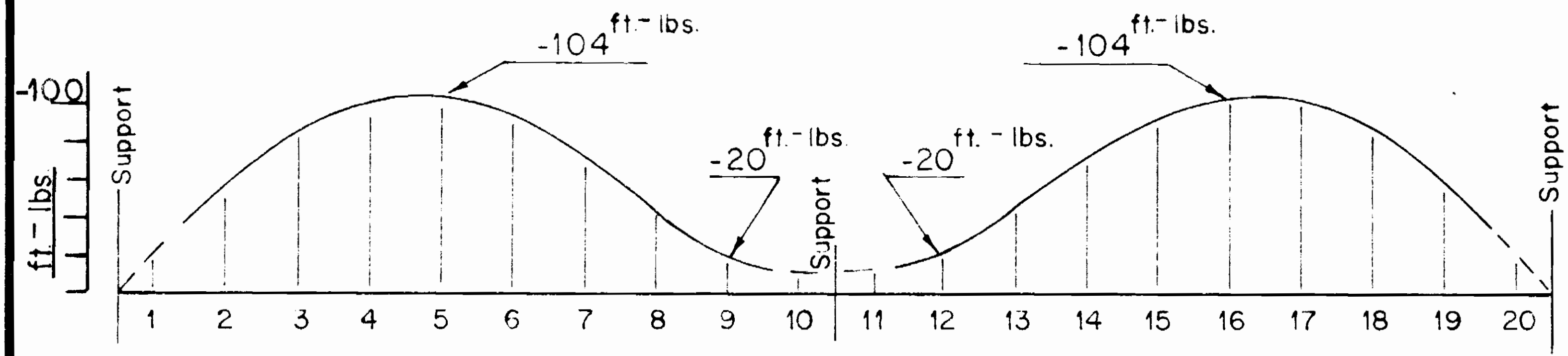

FIGURE 28. EXAMPLE 2 – LONGITUDINAL DISTRIBUTION OF TRANSVERSE BENDING MOMENT (TM''_{jm}) – FOLD LINE C

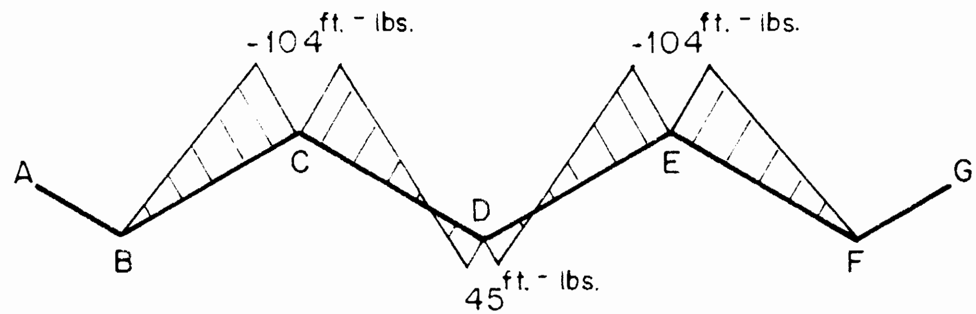

FIGURE 29. EXAMPLE 2 – TRANSVERSE DISTRIBUTION OF TRANSVERSE BENDING MOMENT (TM''_{jm}) – SEGMENT 5

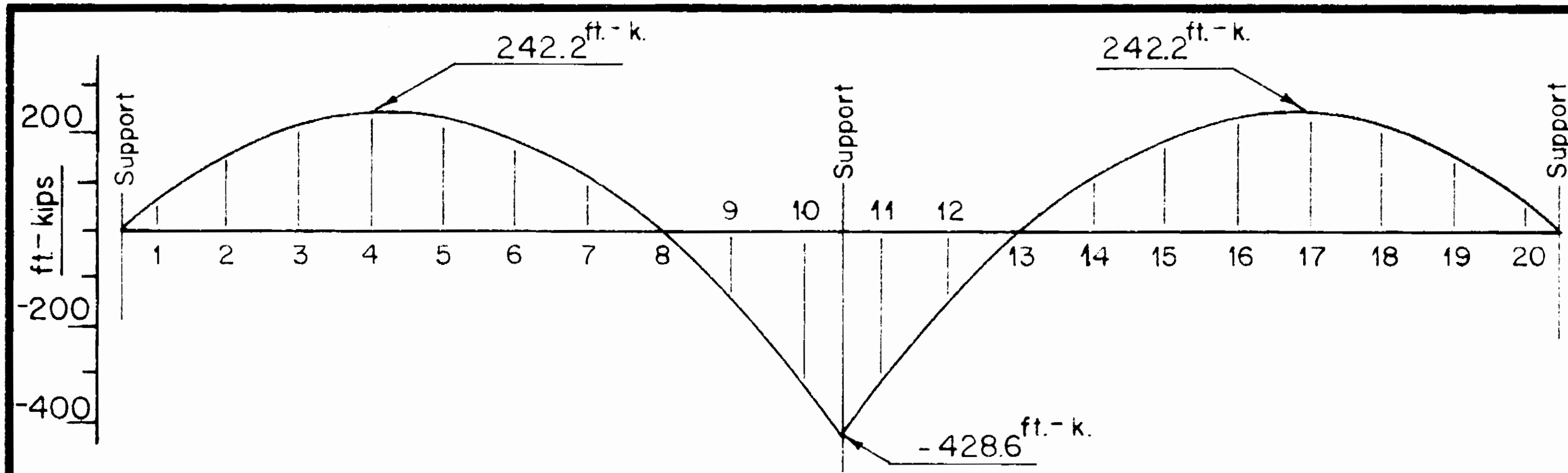

FIGURE 30. EXAMPLE 2 - LONGITUDINAL DISTRIBUTION OF LONGITUDINAL BENDING MOMENT (LM''_{im}) - PLATE 2

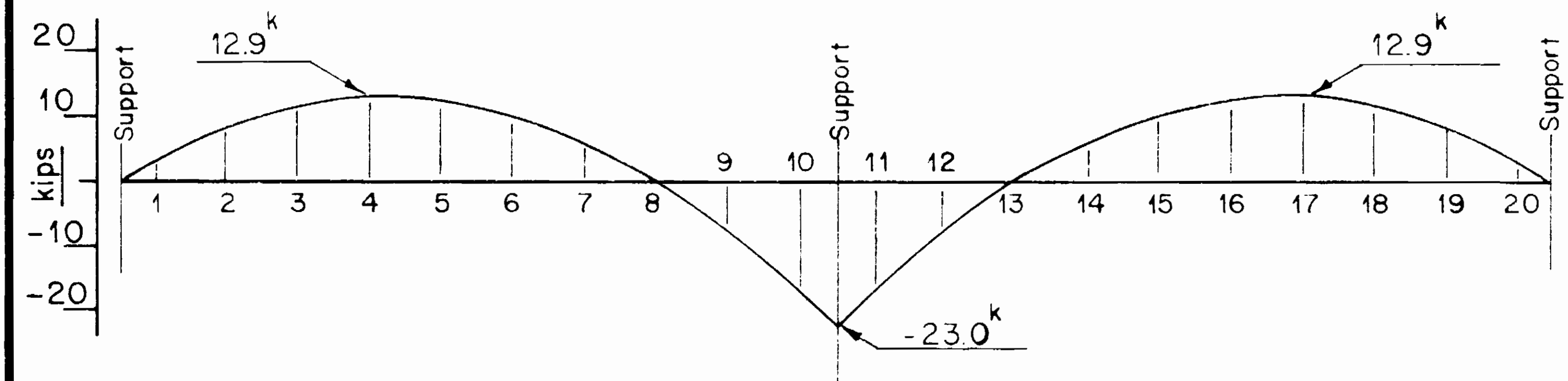

FIGURE 31. EXAMPLE 2 - LONGITUDINAL DISTRIBUTION OF EDGE SHEAR FORCE (N''_{jm}) - FOLD LINE B

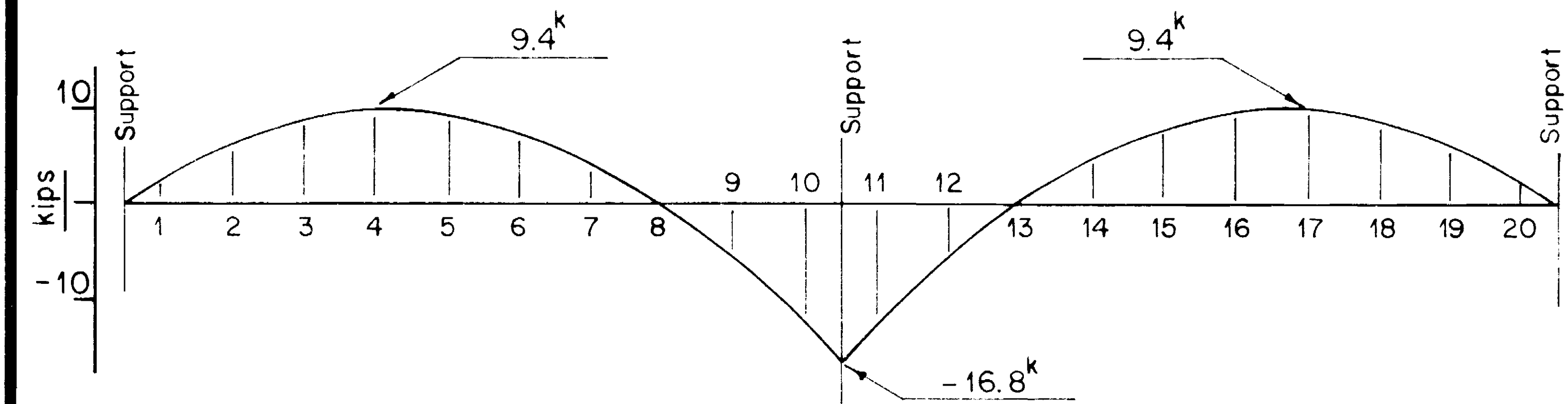

FIGURE 32. EXAMPLE 2 — LONGITUDINAL DISTRIBUTION OF AXIAL PLATE FORCE (P''_{im}) — PLATE 2

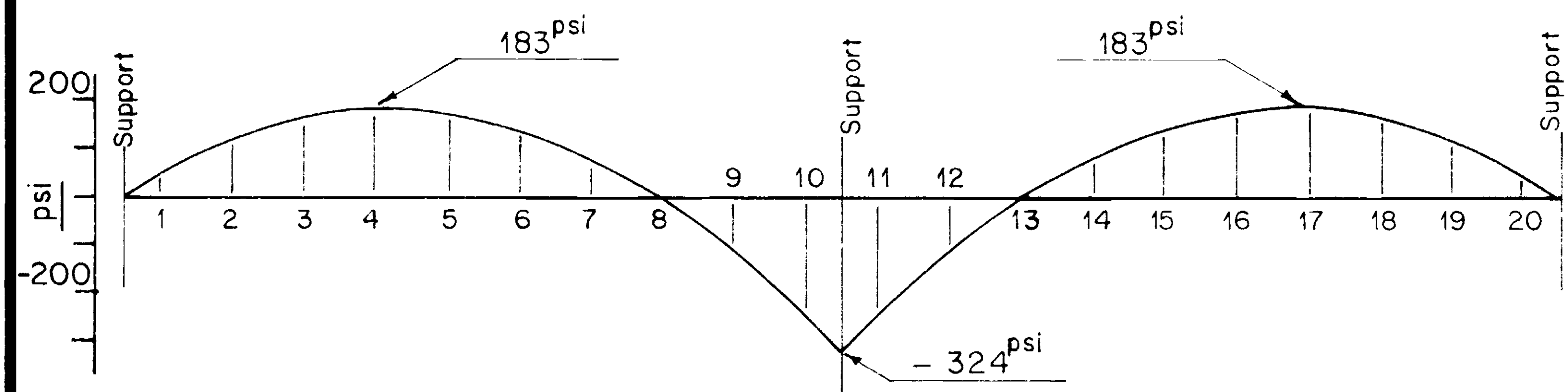

FIGURE 33. EXAMPLE 2 — LONGITUDINAL DISTRIBUTION OF LONGITUDINAL STRESS (f''_{jm}) - FOLD LINE B

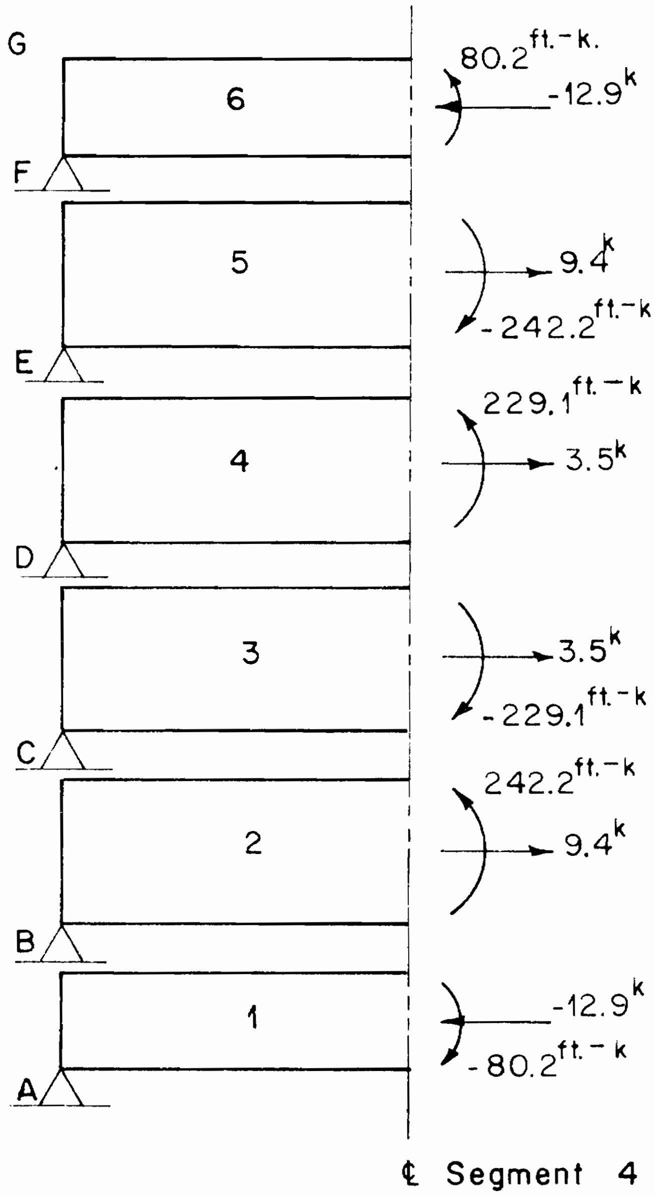

FIGURE 34. EXAMPLE 2 — AXIAL PLATE FORCES (P''_{im}) AND LONGITUDINAL BENDING MOMENTS (LM''_{im}) — SEGMENT 4

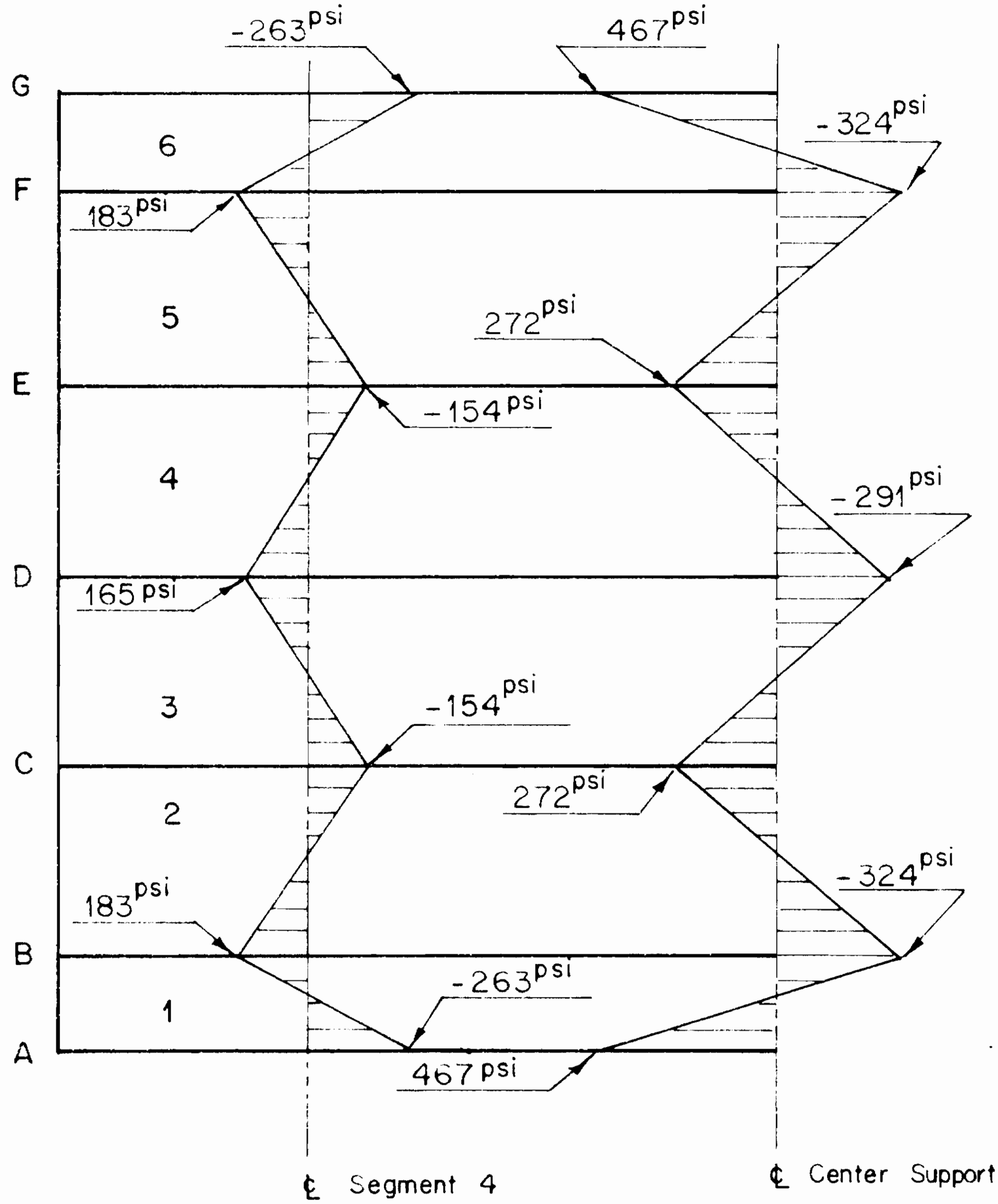

FIGURE 35. EXAMPLE 2 — TRANSVERSE DISTRIBUTION OF LONGITUDINAL STRESSES (f''_{jm})

VIII CONCLUSION

Using familiar techniques of structural analysis and present techniques for analyzing the simply supported, single-span folded plate surface, a general method of analysis of simple or continuous span folded plate surfaces, with general end conditions, has been developed in this dissertation for the solution of the behavior of the folded plate surface for any load condition.

With present techniques for analyzing the folded plate surface, the compatibility in the behavior of the surface in both the transverse and longitudinal directions at the fold lines is provided for at one section in the span and is assumed to be satisfied at all other sections by expressing the deflected shape of the surface and the distribution of the forces and moments in terms of an idealized curve. For the analysis of the continuous-span folded plate surface, present techniques consider each span individually, assuming idealized end conditions, i.e., fixed, free or simply supported. Continuity of the surface over the supports is assured by assuming fixity, but because of this artificial restraint the method of analysis offers only an approximate solution. Within the limitations of the assumptions, the general method of analysis presented in this dissertation gives an "exact" solution for the structural action of the simple or continuous folded plate surface. This general method is based upon a difference technique in which the surface is divided into segments and the compatibility of the surface is insured at the center of each segment as well as at the line of supports and continuity of the surface is maintained over the supports. Thus, the "exact" deflected shape of the surface and the distribution of internal forces, moments and stresses is established. The degree of accuracy of the solution is dependent upon the size of segments chosen; smaller segments provide greater accuracy.

Although the general method of analysis is not convenient for hand calculations, it is readily programmed for the electronic digital computer to analyze the behavior of any folded plate surface under the action of any load condition.

The solution of the structural action of a simple folded plate surface by the general method of analysis has been verified by a comparison with solutions obtained by present techniques of analysis, and the solutions for both single-span and continuous-span surfaces have been verified experimentally.

The experimental investigation of the behavior of the folded plate surfaces of four aluminum models has established excellent verification of the general method of analysis. Tests were conducted on both simply supported, single-span and continuous-span surfaces and very good agreement between the experimental and theoretical values of longitudinal stress and transverse moment were obtained. An examination of the data presented in Appendix C and Figures 18 through 23 shows that for about 80% of the cases the differences between theoretical and experimental values were within ± 15%. A detailed evaluation of the experimental results is given in Sections

VI-D and E.

During the testing of the two-span, continuous surface, it was found that a relative movement of the center support with respect to the end supports of only L/5000 had a major effect on the behavior of the surface. It should be pointed out that there is a definite need for an experimental and theoretical study to establish allowable limits for the control of relative support settlement since this is a problem that will be encountered in practice.

One of the basic assumptions of the general method of analysis presented here is that one-way slab action between fold lines extends the full length of the surface and that the influence of the supporting diaphragms can be neglected. As one would expect, the experimental investigation has indicated that two-way slab action does occur in the vicinity of the supports and that the area of influence of this action extends approximately one half the width of the plate on either side of the support.

There is still a need for additional research in the development of an understanding of the behavior of the continuous folded plate surface, and the general method of analysis presented here can be a valuable tool. In addition, the general method of analysis now makes it possible for the engineer to obtain a solution to the structural behavior of the continuous folded plate surface as an aid to design.

IX ACKNOWLEDGMENT

The author wishes to express his sincere appreciation to his major advisor, Dr. George A. Gray, Professor, Department of Civil Engineering, Virginia Polytechnic Institute, for his assistance, advice and criticism in the preparation of this dissertation, and for his encouragement and guidance over the past four years.

Also, the author wishes to thank the Department of Civil Engineering, Virginia Polytechnic Institute, for financing this research.

X BIBLIOGRAPHY

1. Ehlers, G., "Ein neues Konstruktionsprinzip," Bauingenieur, Vol. 9, 1930, p. 125.

2. Craemer, H., "Theorie der Faltwerke," Benton und Eisen, Vol. 29, 1930, p. 276.

3. Gruber, E., "Berechnung Prismatisch Scheibenwerke," International Association of Bridge and Structural Engineering Memoires, Vol. 1, 1932, p. 225.

4. Gruning, G., "Die Nebenspannungen in Prismatischen Faltwerken," Ingenieur-Archiv., Vol. 3, No. 4, 1932.

5. Vlassow, W. Z., "Structural Mechanics of Shells," (in Russian), Moskwa, 1936.

6. Winter, G. and Pei, M., "Hipped plate Construction," Journal, American Concrete Institute, Vol. 18, No. 5, January, 1947, pp. 505 - 532.

7. Gaafar, I., "Hipped Plate Analysis Considering Joint Displacement," Transactions, American Society of Civil Engineers, Paper No. 2696, Vol. 119, 1954, p. 743.

8. Simpson, H., "Design of Folded Plate Roofs," Proceedings, American Society of Civil Engineers, Paper No. 1508, Vol. 84, January, 1958.

9. Portland Cement Association, "Direct Solution of Folded Plate Concrete Roofs," 1960.

10. Meek, J. L., "Matrix Derivation of the Folded Plate Equations,"

Proceedings, American Society of Civil Engineers, Vol. 89, ST3, 1963, pp. 77 - 105.

11. Barker, R. M., "Folded Plate Analysis Using a Digital Computer and Experimental Model Studies," thesis presented to the University of Minnesota, June, 1962.

12. Scordelis, A. C., "Matrix Formulation of the Folded Plate Equations," Proceedings, American Society of Civil Engineers, Vol. 86, ST10, 1960, pp. 1 - 22.

13. Scordelis, A. C., Cory, E. L. and Stubbs, I. R., "Experimental and Analytical Study of a Folded Plate," Proceedings, American Society of Civil Engineers, Vol. 87, ST8, 1961, pp. 139 - 160.

14. Yitzhaki, D., Prismatic and Cylinderical Shell Roofs, Haifa Science Publishers, Hafia, Israel, 1958.

15. Yitzaki, D. and Reiss, M., "Analysis of Folded Plates," Proceedings, American Society of Civil Engineers, Vol. 88, ST5, 1960, pp. 107 - 142.

16. Sharma, S. P. and Goyal, B. K., "The Analysis of Continuous Folded Plates," Indian Concrete Journal, Vol. 37, No. 12, December, 1963, pp. 448 - 453.

17. Task Committee on Folded Plate Construction, "Phase I Report on Folded Plate Construction," Proceedings, American Society of Civil Engineers, Vol. 89, ST6, 1963, pp. 365 - 406.

18. Gesund, H., "Folded Plates," Chapter 7, Art. 7-2 and 7-3, Advanced Design of Reinforced Concrete, by Dunham, C. W., McGraw-Hill Book Company, New York, 1964.

XI VITA

Frederick William Beaufait, born on November 28, 1936, received his elementary and high school education in the public schools of Vicksburg, Mississippi. In 1954, he entered Mississippi State University to begin the study of civil engineering and was graduated in June, 1958.

After graduation from Mississippi State University, he was employed by the Vicksburg District, U. S. Army Corps of Engineers, as a structural engineer in the Navigation Design Section.

In February, 1959, he entered the University of Kentucky Graduate School to begin working on a Master's degree in structural engineering. While studying at the University of Kentucky, he worked part-time for L. E. Gregg and Associates, Consulting Engineers, and taught part-time in the Civil Engineering Department. Upon completion of study at the University of Kentucky, he participated in an exchange program between the University of Kentucky and the University of Liverpool, Liverpool, England, for the academic year 1960-1961 as a visiting lecturer.

In September, 1961, he entered Virginia Polytechnic Institute to begin study toward the degree of Doctor of Philosophy. While at Virginia Polytechnic Institute, he was a half-time instructor in the Civil Engineering Department.

Fred Beaufait

APPENDIX A - NOTATIONS

The following symbols have been adopted for use in this dissertation:

a_j	=	deflection angle between adjacent plates at fold line j;
d_{im}, d^n_{im}, d''_{im}	=	in-plane deflection of plate i, center of segment m -- membrane analysis, arbitrary rotation of plate n and final solution, respectively;
f_{jm}, f^n_{jm}, f''_{jm}	=	longitudinal fiber stress at fold line j, center of segment m -- membrane analysis, arbitrary rotation of plate n and final solution, respectively;
f_l	=	longitudinal stress, experimental;
f_t	=	transverse stress, experimental;
E	=	modulus of elasticity;
F_{ji}	=	component of edge load (R'_j) at fold line j in the plane of plate i;
F_i	=	sum of components of edge loads (F_{ji}) in the plane of plate i;
I_i	=	moment of inertia of the transverse section of plate i about a centroidal axis normal to the plate;
k_n	=	constant coefficients combining the arbitrary plate rotations and membrane analysis;

l_i = width of plate i;

L_q = length of longitudinal span q;

LM_{im}, LM^n_{im}, LM''_{im} = total longitudinal, in-plane bending moment in plate i, center of segment m -- membrane analysis, arbitrary rotation of plate n and final solution, respectively;

M_{im}, M^n_{im}, M''_{im} = longitudinal, beam bending moment due to beam action in plate i, center of segment m -- membrane analysis, arbitrary rotation of plate n and final solution, respectively;

N_{jm}, N^n_{jm}, N''_{jm} = edge shear force along fold line j, center of segment m -- membrane analysis, arbitrary rotation of plate n and final solution, respectively;

P^N_i , P^T_i = normal and tangential components of applied load an plate i, respectively;

PL_i = total in-plane plate load of plate i;

P_{im} = axial load in plate i, center of segment m;

r_i = final rotation of plate i;

r'_i = arbitrary rotation of plate i;

R_j = reactive force in imaginary support at fold line j;

R'_j = edge load at fold line j;

s_j = shear stress along fold line j;

SM_{ik}, SM^{n}_{ik}, $SM^{''}_{ik}$ = longitudinal, beam bending moment in plate i, support k -- membrane analysis, arbitrary rotation of plate n and final solution, respectively;

TM_{j} = transverse bending moment due to slab action at fold line j for unit strip;

TM_{jm}, TM^{n}_{jm}, $TM^{''}_{jm}$ = transverse bending moment due to slab action at fold line j, center of segment m -- membrane analysis, arbitrary rotation of plate n and final solution, respectively;

t_{i} = thickness of plate i;

ϵ_{l} = average longitudinal strain, experimental;

ϵ_{t} = average transverse strain, experimental;

$\Delta^{'}_{i}$ = relative displacement of edges of plate i for arbitrary rotation of plate i;

Δ_{i} = final relative displacement of edges of plate i;

μ = Poisson's ratio.

APPENDIX B - FLOW CHART

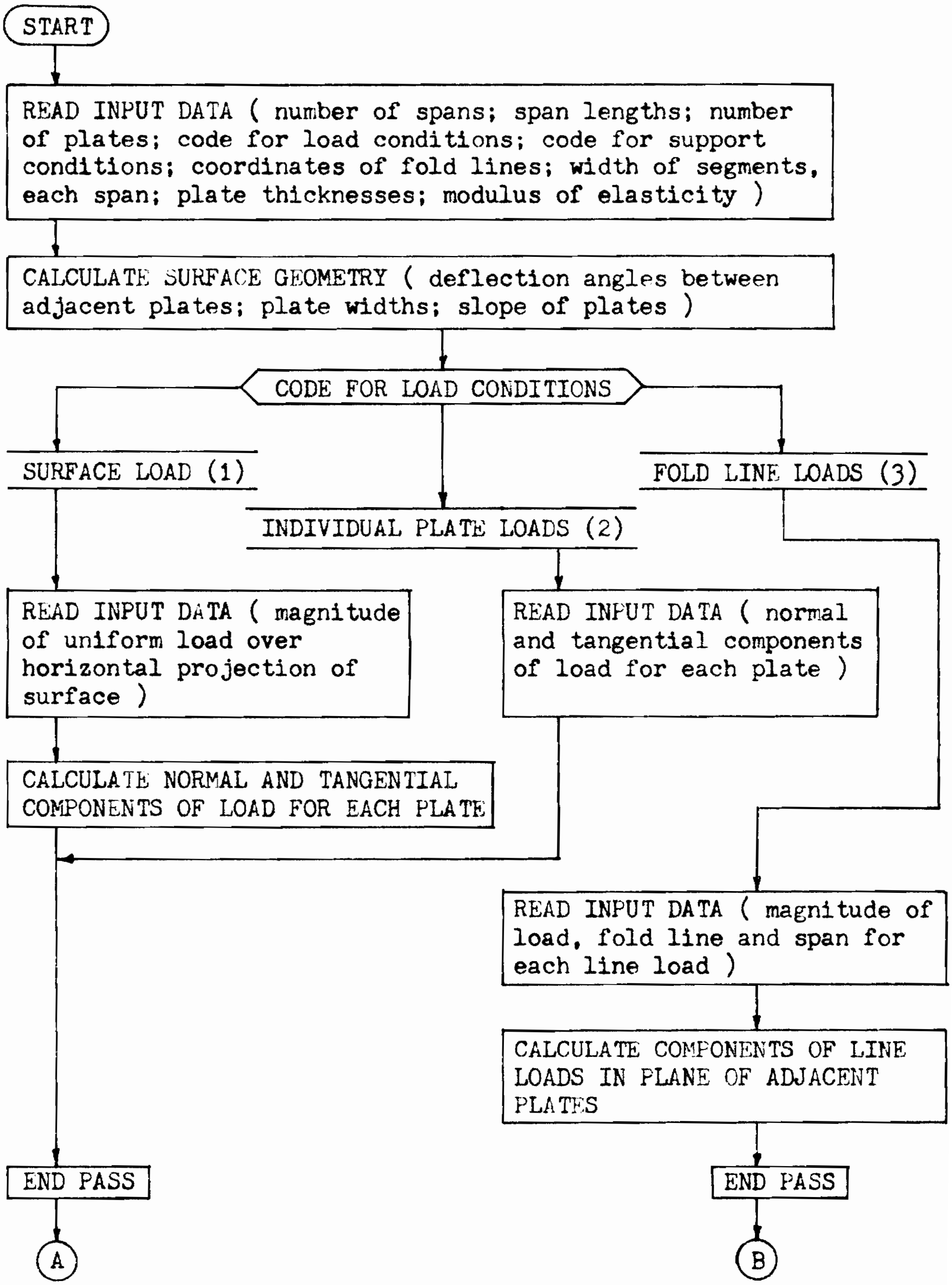

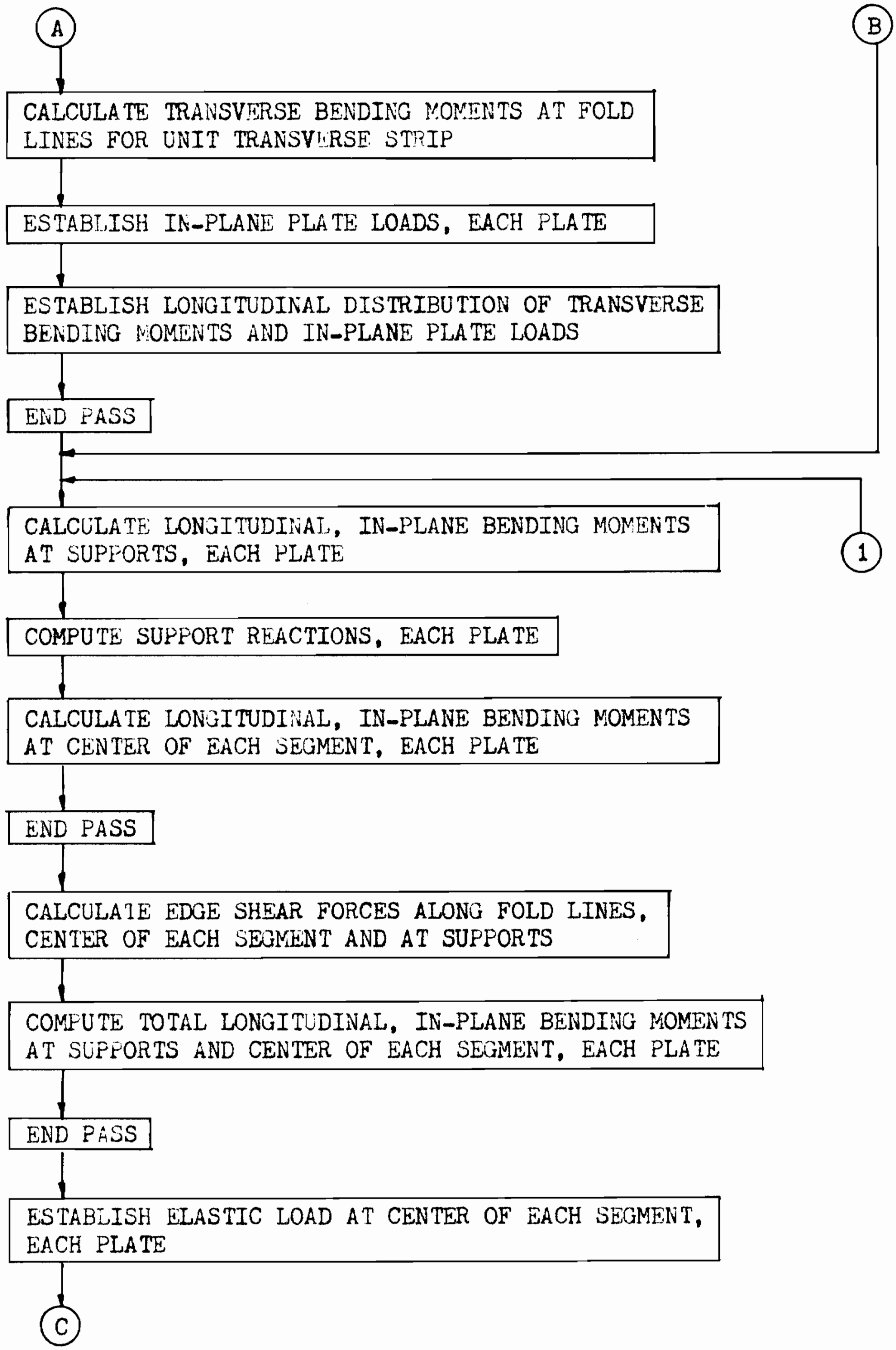
A
B
CALCULATE TRANSVERSE BENDING MOMENTS AT FOLD LINES FOR UNIT TRANSVERSE STRIP
ESTABLISH IN-PLANE PLATE LOADS, EACH PLATE
ESTABLISH LONGITUDINAL DISTRIBUTION OF TRANSVERSE BENDING MOMENTS AND IN-PLANE PLATE LOADS
END PASS
CALCULATE LONGITUDINAL, IN-PLANE BENDING MOMENTS AT SUPPORTS, EACH PLATE
1
COMPUTE SUPPORT REACTIONS, EACH PLATE
CALCULATE LONGITUDINAL, IN-PLANE BENDING MOMENTS AT CENTER OF EACH SEGMENT, EACH PLATE
END PASS
CALCULATE EDGE SHEAR FORCES ALONG FOLD LINES, CENTER OF EACH SEGMENT AND AT SUPPORTS
COMPUTE TOTAL LONGITUDINAL, IN-PLANE BENDING MOMENTS AT SUPPORTS AND CENTER OF EACH SEGMENT, EACH PLATE
END PASS
ESTABLISH ELASTIC LOAD AT CENTER OF EACH SEGMENT, EACH PLATE
C

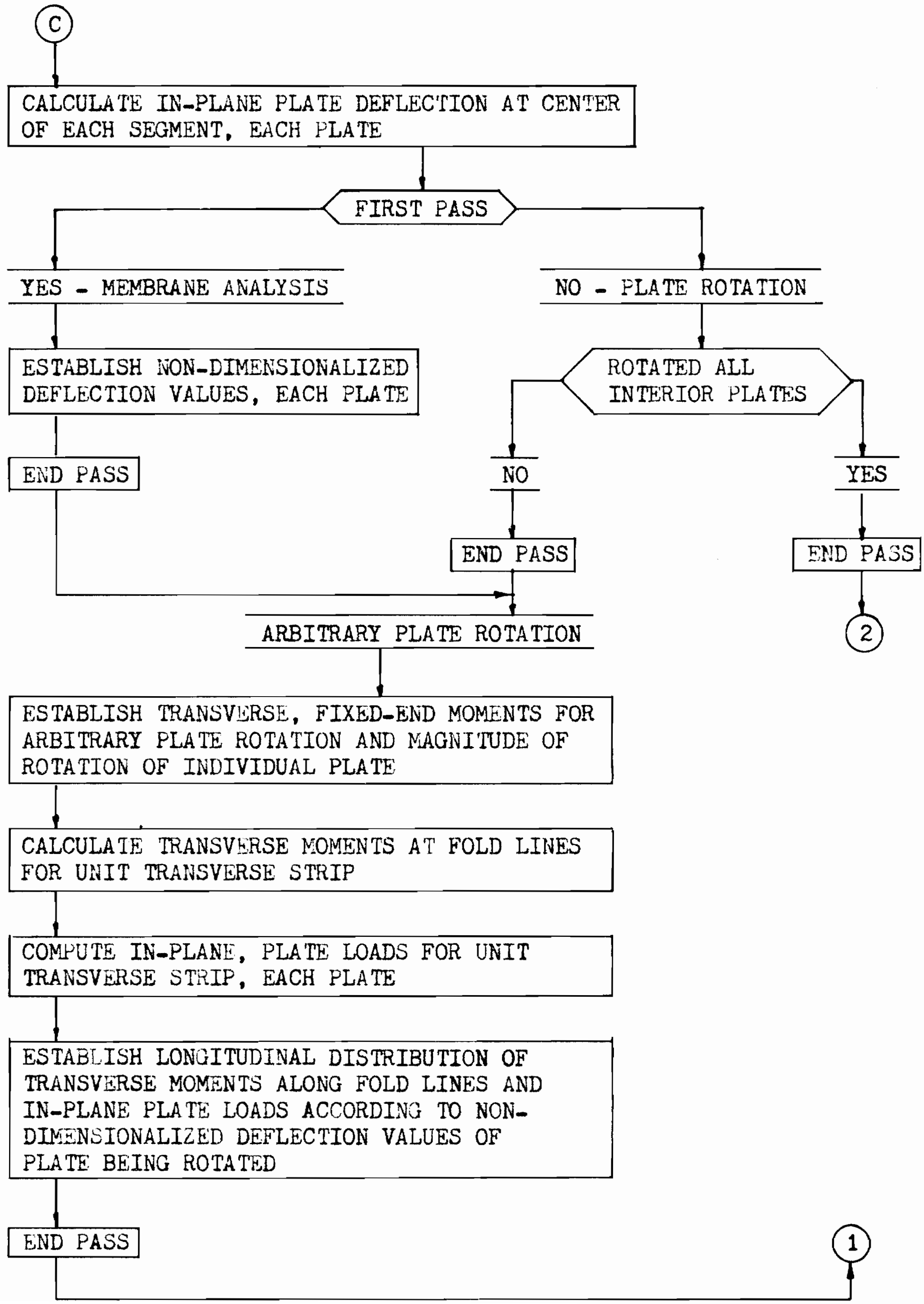
C
CALCULATE IN-PLANE PLATE DEFLECTION AT CENTER OF EACH SEGMENT, EACH PLATE
FIRST PASS
YES - MEMBRANE ANALYSIS
NO - PLATE ROTATION
ESTABLISH NON-DIMENSIONALIZED DEFLECTION VALUES, EACH PLATE
ROTATED ALL INTERIOR PLATES
END PASS
NO
YES
END PASS
END PASS
2
ARBITRARY PLATE ROTATION
ESTABLISH TRANSVERSE, FIXED-END MOMENTS FOR ARBITRARY PLATE ROTATION AND MAGNITUDE OF ROTATION OF INDIVIDUAL PLATE
CALCULATE TRANSVERSE MOMENTS AT FOLD LINES FOR UNIT TRANSVERSE STRIP
COMPUTE IN-PLANE, PLATE LOADS FOR UNIT TRANSVERSE STRIP, EACH PLATE
ESTABLISH LONGITUDINAL DISTRIBUTION OF TRANSVERSE MOMENTS ALONG FOLD LINES AND IN-PLANE PLATE LOADS ACCORDING TO NON-DIMENSIONALIZED DEFLECTION VALUES OF PLATE BEING ROTATED
END PASS
1

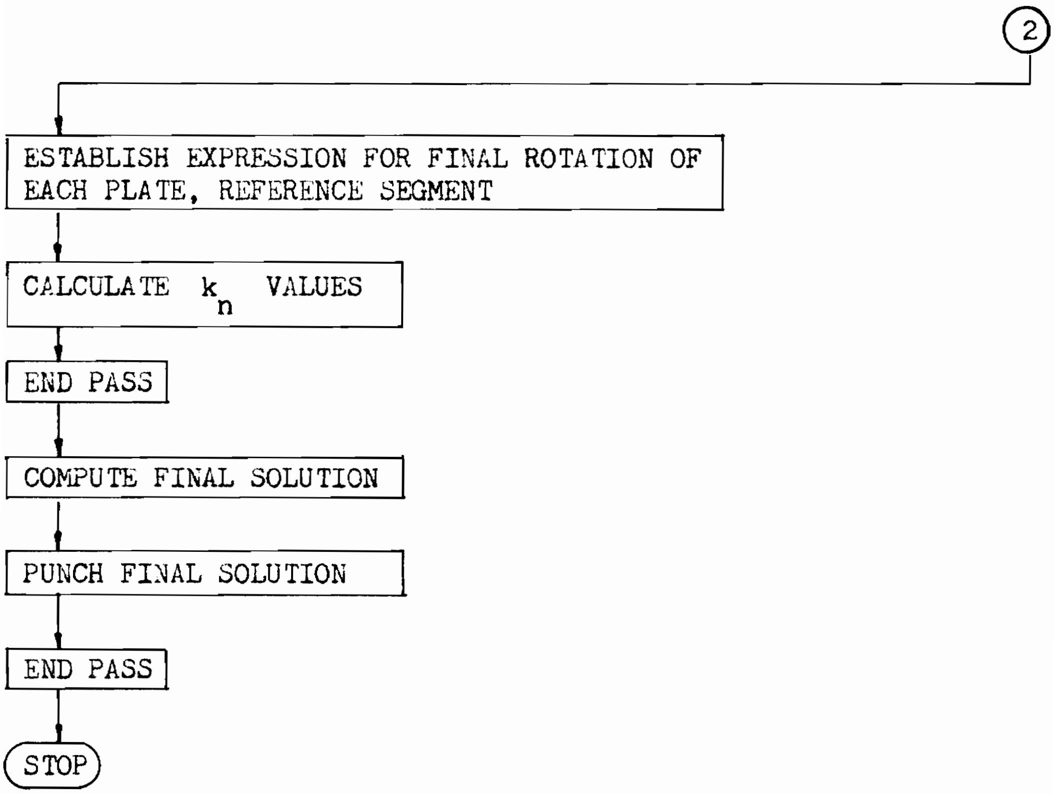
2
ESTABLISH EXPRESSION FOR FINAL ROTATION OF EACH PLATE, REFERENCE SEGMENT
CALCULATE k_n VALUES
END PASS
COMPUTE FINAL SOLUTION
PUNCH FINAL SOLUTION
END PASS
STOP

APPENDIX C - EXPERIMENTAL DATA

Odd numbered gages - longitudinal direction

Even numbered gages - transverse direction

TABLE 4 MODEL 1 - EXPERIMENTAL DATA

Gage	Experimental Strain in./in. x 10^{-6}	Theoretical Strain in./in. x 10^{-6}	Difference	f_l psi	f_t psi
1	31	33	2	-309	
2	-14	-11	3		----
3	29	33	4	-309	
4	-10	-11	1		----
5	-13	-15	2	-131	
6	6	5	7		0
7	-17	-15	2	-202	
8	1	5	3		- 60
9	-19	-14	5	-238	
10	- 2	- 5	3		- 95
11	-18	-21	3	-154	
12	15	16	1		107
13	-16	-11	5	-426	
14	-61	-82	21		-795
15	-16	-18	2	59	
16	63	93	30		690

TABLE 5 MODEL 2 - EXPERIMENTAL DATA

Gage	Experimental Strain in./in. x 10^{-6}	Theoretical Strain in./in. x 10^{-6}	Difference	f_l psi	f_t psi
1	-49	-48	1	-523	
2	15	16	1		- 12
3	-49	-48	1	-535	
4	14	16	2		- 24
5	12	13	1	131	
6	- 3	- 4	1		12
7	12	13	1	119	
8	- 7	- 4	3		- 36
9	29	23	6	356	
10	4	9	5		166
11	26	36	10	214	
12	-23	-29	6		-166
13	-21	-30	9	-119	
14	33	38	5		309
15	-20	- 9	11	-332	
16	-23	-25	2		-356
17	-26	-27	1	-238	
18	19	19	0		119
19	-23	-19	4	-261	
20	- 3	- 4	1		-131
21	-22	-31	9	-131	
22	33	39	6		309
23	-21	-10	11	-345	
24	-23	-25	2		-356
25	28	35	7	356	
26	7	8	1		190
27	27	23	4	226	
28	-24	-27	3		-178

TABLE 6 MODEL 3 - EXPERIMENTAL DATA

Gage	Experimental Strain in./in. x 10^{-6}	Theoretical Strain in./in. x 10^{-6}	Difference	f_l psi	f_t psi
1	-37	-35	2	-392	
2	13	11	2		12
3	-33	-35	2	-345	
4	12	11	1		12
5	11	10	1	119	
6	- 2	- 3	1		24
7	13	10	3	131	
8	- 5	- 3	2		- 12
9	18	16	2	226	
10	3	3	0		107
11	22	22	0	202	
12	-14	-15	1		- 83
13	-13	-24	11	- 24	
14	32	37	5		332
15	-13	- 3	10	-250	
16	-25	-28	3		-344
17	-13	-24	11	- 24	
18	34	37	3		356
19	-13	- 3	10	-238	
20	-22	-28	6		-309
21	20	16	4	262	
22	6	3	3		155
23	21	22	1	178	
24	-18	-15	3		-131

TABLE 6 - CONTINUED

Gage	Experimental Strain in./in. x 10^{-6}	Theoretical Strain in./in. x 10^{-6}	Difference	f_1 psi	f_t psi
25	23	23	0	250	
26	- 5	- 8	3		36
27	19	23	4	202	
28	- 6	- 8	2		0
29	- 7	-12	5	-202	
30	-31	4	27		-380
31	4	-12	16	166	
32	30	4	26		368
33	- 6	- 4	2	-286	
34	-53	1	52		-655
35	13	- 4	17	321	
36	43	1	42		559
37	2	5	3	- 95	
38	-30	- 2	28		-344
39	9	5	4	226	
40	32	- 2	34		416
41	8	6	2	83	
42	- 3	0	3		0
43	6	7	1	60	
44	- 4	- 4	0		- 24

TABLE 7 - MODEL 4 - EXPERIMENTAL DATA

Gage	Experimental Strain in./in. x 10^{-6}	Theoretical Strain in./in. x 10^{-6}	Difference	f_1 psi	f_t psi
1	-25	-26	1	-262	
2	9	9	0		12
3	-20	-26	6	-202	
4	9	9	0		24
5	9	10	1	95	
6	- 3	- 3	0		0
7	12	10	2	131	
8	- 2	- 3	1		24
9	13	9	4	190	
10	8	8	0		143
11	16	17	1	131	
12	-14	-17	3		-107
13	- 9	-20	11	24	
14	32	35	3		344
15	-10	- 1	9	-214	
16	-25	-28	3		-333
17	-10	-20	10	- 12	
18	28	35	7		297
19	- 9	- 1	8	-202	
20	-25	-28	3		-333
21	25	20	5	273	
22	- 7	- 6	1		12
23	24	20	4	262	
24	- 7	- 6	1		12

TABLE 7 - CONTINUED

Gage	Experimental Strain in./in. x 10^{-6}	Theoretical Strain in./in. x 10^{-6}	Difference	f_l psi	f_t psi
25	-11	-10	1	- 95	
26	8	4	4		48
27	-12	-10	2	-119	
28	5	3	2		12
29	8	4	4	190	
30	25	32	7		333
31	8	19	11	- 36	
32	-33	-36	3		-357
33	51	41	10	546	
34	-15	-13	2		24
35	43	41	2	451	
36	-15	-13	2		- 12
37	-22	-19	3	-238	
38	6	5	1		- 12
39	-23	-20	3	-226	
40	11	8	3		36
41	16	3	13	238	
42	11	29	18		190
43	16	25	9	107	
44	-21	-38	17		-190
45	12	9	3	166	
46	7	8	1		131
47	14	17	3	107	
48	-15	-17	2		-119

ANALYSIS OF CONTINUOUS FOLDED PLATE SURFACE

ABSTRACT

A general method of analysis is developed for the solution of single or continuous span folded plate surfaces, with general end conditions, for any load. By considering the folded plate surface as a single, longitudinal unit throughout the analysis, the continuity of the surface is maintained over transverse supports. Within the limitations of the assumptions, this method yields an "exact" solution of the structural action based upon a difference technique in which the surface is divided into segments: combatibility of the surface is insured at the center of each finite segment along the span and over the supports.

A computer program for the analysis of simply supported, single-span and continuous-span folded plate surfaces, with and without overhangs at each end, under three load conditions is described. A comparison is made between this general method of analysis and presently accepted techniques; and a final solution for a continuous folded plate surface is presented.

The results of an experimental investigation to study the behavior of four different folded plate structures and to verify the general method of analysis are discussed.